nature portfolio

Peer Review File

Combination of Nanoparticles with Single-Metal Sites Synergistically Boosts Co-Catalyzed Formic Acid Dehydrogenation

REVIEWER COMMENTS

Reviewer #1 (Remarks to the Author):

In the manuscript " Combination of Nanoparticles with Single-Metal Sites Synergistically Boosts Co-Catalyzed Formic Acid Dehydrogenation " Shi et al; have demonstrated that the catalytic performance of hydrogen-generating catalysts can be significantly improved by using materials with both highly distributed single metal sites as well as small defined nanoparticles. The presented catalyst surpasses the activity of defined Co SAs and Pd/C catalysts by 4 and 15 times, respectively. In a broader sense, this study provides design ideas for novel single-metal atom catalysts and deepens the understanding of how the catalytic performance can be enhanced by synergistic action of metal sites of different sizes.
The manuscript is interesting, but they are still at a very premature point of analysis, there is a lack of data to support some of the hypotheses raised. For that main reason and the following points, I propose that it be rejected for publication in Nature Communications.

1. Although the introduction is well written, a real comparison with the most recent results obtained for the dehydrogenation of formic acid in liquid media is lacking.

2. The authors claim in their introduction that one of the great advantages of using such materials, instead of the already known and industrially used materials, is the cost reduction due to the fact that they are not based on noble metals. However, this type of catalyst is based on a hierarchically structured material with a zeolitic structure, which is subsequently pyrolysed with a relatively low yield. In this sense, this reviewer has two recurring questions, the first is could the authors determine the final yield in the synthesis of the catalyst, based on the final weight loss involved in the pyrolysis process. And the second is, have the authors carried out a market study to determine the price per kilogram of catalyst obtained? In this way, a fairer comparison can be made with the commercial catalyst and its potential can be highlighted.

3. There is some discrepancy in the process of catalyst synthesis. In the supporting info, the authors say that the catalysts have been pyrolysed in an inert atmosphere (Argon), however, in the discussion of results the authors say that the pyrolysis atmosphere is a reducing atmosphere (6%H2 Ar balance), Line 110. If this is the case, how can the catalyst be reduced in an inert atmosphere during pyrolysis?
4. Furthermore, the samples seem to be pyrolysed at different temperatures, 750, 850 and 950ºC in the manuscript and 800, 900 and 1000ºC in the supporting information. Please clarify this error and describe the process accordingly.

5. The XRD of the presented catalysts have a very high noise-to-signal ratio, which makes it difficult to assign cobalt metal peaks to an amorphous carbon peak. The authors should repeat these XRDs with a higher step number to increase their resolution.

6. The authors should add the cobalt particle size distributions found for the catalysts to the manuscript. It seems that, with increasing pyrolysis temperature, these distributions become wider.

7. Elemental analysis of the samples should be done to evaluate the percentage of nitrogen, oxygen, carbon and hydrogen in the samples.

8. It seems contradictory, that the authors show particles measured in HAADF-STEM, for all three catalysts, Figure 1c and Figure s6, with sizes clearly below 500 pm, yet they are able to see a peak associated with metallic cobalt by XRD. How is this possible?

9. It is strange that the 002 peak for amorphous carbon in the XRD is more crystalline for the sample pyrolysed at 850 than for the sample pyrolysed at 950C. This would indicate that the sample pyrolysed at 850C is more graphitic than the sample pyrolysed at the higher temperature? The authors should calculate the R and Lc values, following the approach of Alexander et al. for all catalysts (L. E. Alexander and E. C. Sommer, J. Phys. Chem., 1956, 60, 1646–1649).

10. This author does not entirely agree with this statement, “The similar cobalt content in the three catalysts suggests that the coordination structure of the active site rather than the metal content is responsible for the differences in performance, as discussed below” as it has been extensively studied and published for this reaction, that not only the metal loading is responsible, but also the particle size of the metal. It has been found that the reaction is structure-sensitive. (Chemical Engineering Journal 420 (2021) 127641, J. Catal. 352 (2017) 371–381, CS Appl. Mater. Interfaces 9 (2017) 24678–24687, ChemistrySelect 1 (2016) 1879–1886).

11. This author disagrees with this statement, “All these results indicate that atomically dispersed Co sites and N-doped graphite-encapsulated nanoparticles are successfully anchored on NC carriers in Co-SAs/NPs@NC-950, whereas only single metal sites are present in the other samples”, for many reasons. First of all, there is no evidence of graphite in the samples, since the XRD of all samples show broad, undefined peaks characteristic of amorphous carbons and not graphite. Secondly, the sample calcined at a higher temperature shows a lower proportion of nitrogen groups, as the authors claim in the paragraph below. That is why the number of NC carriers in this sample should be lower than in the others. And consequently, the anchoring of the weaker active phase, results in greater sintering of the cobalt particles.

12. What is the effect of zinc on the stabilization of cobalt particle size? According to the synthesis procedure, the same amount of zinc nitrate as methylimidazole is added at the beginning of the synthesis. Are there traces of zinc in the pyrolyzed catalyst? The effect of possible zinc remaining in the catalyst after pyrolysis must be added to the discussion of the results. At the same time, the study of the loading of the different metals of the catalyst by ICP is required for the discussion of the results.

13. The general XPS spectrum and the zinc and oxygen spectrum should be added to the manuscript for discussion, as well as a table with the atomic percentages for each species.

14. The XPS spectra of the manuscript should be generally reviewed and corrected. The assignment and deconvolution of the cobalt XPS spectrum should be reviewed. The assignment for the Co-N species, (781.6 eV from NIST), appears to be shifted to lower binding energy for the 750 and 850 C samples. Likewise, the width of the peak assigned to graphitic N in the nitrogen spectrum is much higher than that of the rest of the peaks.

15. Authors claim that "The observed formic acid dehydrogenation activities under the same conditions were in the order of Co-SAs/NPs@NC-950 > Co SAs > Co NPs, showing that the atomically dispersed CoN2C2 sites are more active than NPs. Could these differences be attributed to the presence of zinc in the samples?

16. Equation S3 of supporting info is poorly described. To calculate the turnover frequency, TOF, the authors must calculate the number of moles of H2, divide it by the number of total moles of Co, and the reaction time. The TOF values should be recalculated to compare with the literature.

17. Equation S6 is incorrectly calculated and if the selectivity has been calculated following this equation, it must be recalculated again. The selectivity towards hydrogen should be Volume of hydrogen, divided by the volume of hydrogen, carbon monoxide and carbon dioxide.

18. There are figures that on a scientific level do not contribute anything to the manuscript, such as figures S1, S2, S3, and S17. They could be removed from the supporting information, without compromising the essential information.
For this reason, the work might not be published in Nature communications.

Reviewer #2 (Remarks to the Author):

Review: NCOMMS-24-08249: Combination of Nanoparticles with Single-Metal Sites Synergistically Boosts Co-Catalyzed Formic Acid Dehydrogenation

The manuscript entitled Combination of Nanoparticles with Single-Metal Sites Synergistically Boosts Co-Catalyzed Formic Acid Dehydrogenation is a very interesting article as the authors claim that nanoparticles and single atoms act synergistically to facilitate the facile dehydrogenation of formic acid, more efficiently than many noble metal catalysts. The introduction of the manuscript is highly informative, places the work in context and justifies the importance of the project and the need to develop new catalyst technology and identify more stable and efficient systems. The work is meticulous and thorough across catalyst preparation, characterisation and catalyst

evaluation/comparison and post catalysis analysis and the results provide a significant advance to the area of catalyst development for hydrogen technologies and as such will be of interest to academic and industrial researchers in allied areas. Overall, the work has been conducted to a very high standard and could be suitable for publication in Nature Communications, if the other reviewers agree, as it reports a new concept in XXX (although synergy between supported SAs and NPs has been reported Adv. Mater. 2022, 34, 2200057, ACS Nano 2021, 15, 9, 14453–14464, Applied Catalysis B: Environmental 2023, 323, 122190) that could represent a significant advance in catalyst discovery for hydrogen storage, as such I recommend publication after addressing the following comments and conducting associated revisions.

1) Define PC at the earliest possible disclosure, presumably in the abstract where it should be described as the optimum solvent.
2) Page 6 ln 107- What happens if you change the Co:Zn ratio in the catalyst synthesis? At the very least the authors should defend their choice of the ratio, but it would be more informative to have some comparative data.
3) Page 8 ln 118- Compare and discuss the surface area and pore size data with other 'related materials' as there are many examples e.g. ChemistrySelect 2022, 7, e202203273. ChemCatChem 2022, 14, e202101472. Scientific Reports 2017, 7, 39789.
4) If the Co-SAs/NPs@NC-750 or 850 catalysts are heated at 950 °C for the appropriate time is the resulting material as active as Co-SAs/NPs@NC-950 and does it have the same textural properties.
5) Page 10 ln 197- least squares
6) Pg 11 ln 204- can the evolution of the catalyst be monitored using VT XRD.
7) Pg 12 ln 222-225- More detail required here on the additional catalysts. How did the composition and textural properties of the catalyst change as a function of the pyrolysis time i.e. can any conclusions be made about why 0.5 h, 1 h and 2 h differ? For instance, N2 adsorption data, XPS and HAADF-STEM should be provided for the catalyst generated after 30 min to explore the difference in performance.
8) Figure S12 – is this the plot for catalyst generated at Co-SAs/NPs@NC-950? if so include catalyst details in the caption.
9) Page 12 ln 234- Fig S13 shows a marked enhance in TOF in the early stages of the reaction with sodium formate as additive (up to ca. 20 min). The authors should comment as it would be an ideal system if the subsequent drop in TOF could be overcome. The caption in Fig S13 should also include the catalyst.
10) Page 12 ln 236- The authors should explain the kinetics of hydrogen release as a function of the catalyst concentration in terms of reaction order and its interpretation. Again, add the catalyst to the caption rather than assume the reader knows.
11) Page 13 ln 241- compare the apparent activation energy to related system in the literature and discuss.
12) Page 15 ln 292- Can the authors describe more clearly what they mean by the carbonate pathway (maybe include a figure) as I understand the formate HC(O)O and thought the other C(O)OH was carboxyl. Please clarify.
13) Page 16 ln 319- Can the authors comment on whether the hydrogen released from DC(O)OH is all HD or a mixture of isotopomers.
14) Pages 18-19- The authors correlate the elevated d band center (to -0.67 eV) with and enhanced

adsorption and activation of intermediates but it's not clear why or how this occurs as C-H cleavage of the formate is the RDS, so how is this facilitated? Its not clear in the TS from the DFT calculations how activation of this C-H occurs and why it is facilitated for the NP system. Is it associated with the depletion of electrons on the Co site?
15) Page 19- relates to the point above (which I accept may reflect my lack of understanding). Could the enhancement in activity for the Co-SAs/NP-950 system be associated with the different coordination environments at the single atom i.e. the C2N2Co rather than the CoN4 associated with the less active catalysts (and thereby not due to the NP other than it is required to change the C/N ratio and thereby the coordination at Co). This does not appear to have been explored by calculations as the Co SAs model was CoN2C2 rather than CoN4. Is it worth performing these calculations to compare?

Reviewer #3 (Remarks to the Author):

Shi et al have reported the dehydrogenation of formic acid utilizing cobalt based single atom catalysts with their activity synergistically increased by combining them with nanoparticles. The catalytic system can be typically considered as a hybrid system consisting of nanoparticles and single-metal sites. Three different set of Co-SAs/NPs@NC were synthesized based on the pyrolysis temperature (750℃, 850℃ and 950℃) and the desired catalytic system having both nanoparticles and single atom catalytic sites were found only in Co-SAs/NPs@NC-950. All the three systems were studied for their catalytic activity and all systems showed better behaviour compared to standard commercial noble metal catalysts (Pd/C and Pt/C) with Co-SAs/NPs@NC-950 providing the best results. The catalyst was found to be stable in long term tests with no significant cobalt leaching. Furthermore, the dehydrogenation v/s dehydration reaction showed selectivity up to 99.96%. The formic acid dehydrogenation mechanism is believed to exclusively follow the formate ion mechanism instead of carbonate ion mechanism based on DRIFT, KIE and DFT studies.

The report provides deep insight into the synergistic effect of nanoparticles on the catalytic activity of cobalt based single atom catalysts for dehydrogenation of formic acid. The results are well supported by experimental and theoretical data and can open new opportunities in understanding how the catalytic performance can be enhanced by synergistic action of metal sites of different sizes.

Based on above mentioned reasons, this manuscript can be published in Nature Communications

Minor corrections:

Page 12: While discussing solvent screening, abbreviation for propylene carbonate (PC) has been directly used and it is not clear which solvent has been used. The authors should mention the name of the solvent instead of directly using the abbreviation form.

Page 7: while discussing cobalt content in 3 different types of catalysts; Co-SAs/NPs@NC-750 should be written after Co-SAs/NPs@NC-850 (in decreasing order of the pyrolysis temperature) as the same trend is followed throughout the whole manuscript

Response to Reviewer 1:

Reviewer 1's comments: In the manuscript " Combination of Nanoparticles with Single-Metal Sites Synergistically Boosts Co-Catalyzed Formic Acid Dehydrogenation " Shi et al; have demonstrated that the catalytic performance of hydrogen-generating catalysts can be significantly improved by using materials with both highly distributed single metal sites as well as small defined nanoparticles. The presented catalyst surpasses the activity of defined Co SAs and Pd/C catalysts by 4 and 15 times, respectively. In a broader sense, this study provides design ideas for novel single-metal atom catalysts and deepens the understanding of how the catalytic performance can be enhanced by synergistic action of metal sites of different sizes.

The manuscript is interesting, but they are still at a very premature point of analysis, there is a lack of data to support some of the hypotheses raised. For that main reason and the following points, I propose that it be rejected for publication in Nature Communications.

Our response: We thank the referee for the comments. We have supplemented HAADF, XRD, Raman and XPS to support the hypothesis of coexistence of nanoparticles and single atoms, the presence of graphitic carbon and the effect of zinc on the reaction.

Complementary HAADF of Co-SAs/NPs@NC-950 samples, combined with XAFS and DFT, confirms our proposed composite structure of nanoparticles and single atoms. Supplementary higher step size XRD and Raman spectroscopy, combined with HRTEM, confirmed the N-doped graphite-like carbon-encapsulated nanoparticle structure in Co-SAs/NPs@NC-950. We compared TEM images of catalysts obtained by pyrolysis of CoZn-ZIF and Co-ZIF, supplemented with Zn content, 2p spectra, and activity tests of Zn-ZIF-8 and Zn-N-C, and found that the presence of Zn had a positive effect on Co nanoparticle size modulation, but did not affect the activity of the cobalt.

Question 1: Although the introduction is well written, a real comparison with the most recent results obtained for the dehydrogenation of formic acid in liquid media is lacking.

Answer: We add a comparison of the liquid-phase formic acid dehydrogenation activity of homogeneous, non-homogeneous noble metal and inexpensive transition metal

catalysts in the revised manuscript. As shown in column 4 of Table S11 and column 2 of the following Table, Generally, noble metal heterogeneous and homogeneous catalysts have higher gas production rates (50-500 times higher) than non-noble metal catalysts.[1, 2] However, considering the cost of the precious metals is more than 1,000 times that of cobalt (e.g., Co: $27,150/t, Pd: $901/t.oz), cobalt-based catalysts have great potential for gas productivity per unit price based on a comparison of the best non-noble Co-N-C catalyst (884.0 $L \cdot h^{-1} \cdot \$^{-1}$) with the noble metal catalysts (See table below for details).[3] Our proposed Co-SAs/NPs@NC-950 reached 1922.1 $L \cdot h^{-1} \cdot \$^{-1}$, which is higher than most of the noble metal catalysts (Pd-based heterogeneous catalysts and Ru-based homogeneous catalysts), and has a promising application (See table below for details).

Table S11. Comparison of the catalytic performance of representative heterogeneous catalysts for the dehydrogenation of formic acid in the liquid phase.

Catalyst	Solvents	Temp (°C)	Gas production rate ($mL \cdot g^{-1} \cdot h^{-1}$)	Selectivity (%)
Co@NC-Gr2	o-xylene	95.5	62.0	99.50
MoS_2/Graphene[a]	/	145	83.3	/
5% Pd/C	PC	98	96.2	/
5% Pt/C	PC	98	147.6	/
Co(1)/Phen(2)/C	PC	98	158.0	/
Co-N-C(NPs)	PC	98	229.2	99.88
γ-Mo_2N/0.2NK-C	H_2O	87	293.9	≈100
Soybean-Mo (0.1)	H_2O	110	293.9	100
Co-N-C(SACs)	PC	98	319.2	99.63
Co(1)/Phen(7)/C	PC	98	423.3	99.80
Co/Cu-N-C	PC	98	1331.2	99.93
Pd-PCN-350R	PC	110	766	/
PF-$Mo_{1.98}C_{1.02}$	H_2O+Sodium formate	100	790	≈100

Pd-PCN-350R	toluene	120	3844	100
Co-SAs/NPs@NC-750	PC	98	257.7	/
Co-SAs/NPs@NC-850	PC	98	557.3	/
Co-SAs/NPs@NC-950	PC	98	1403.8	**99.96**

[a] Catalytic decomposition of formic acid vapors.

Table. Comparison of the gas productivity per unit price of representative noble and non-noble metal catalysts for the dehydrogenation of formic acid.[1, 2]

Catalyst	**TOF (h^{-1})**	**gas productivity per unit price ($L \cdot h^{-1} \cdot \$^{-1}$)**
$[RuCl_2(PPh_3)_3$	2688	100.2
$[RuCl_2(C_6H_6)]_2$/DPPE	47970	1787.9
$[RuCl_2$(benzene)$]_2$/meso-P4	4580	170.7
$[(PNNNP^2)RuH_2(CO)]$	7300	272.1
$[(Cp^*Ir)_2(THBPM)Cl_2]Cl_2$	228000	334.7
[Cp*Ir(L41)Cl]Cl	487500	715.6
[Cp*Ir(pyrimidyl imidazoline)$H_2O]SO_4$	322000	472.6
Pd/N-MSC-30	8414	133.3
Pd@CN900K	14400	228.1
Co-N-C(SACs)	319.2[a]	884.0
Co-SAs/NPs@NC-750	257.7[a]	352.9
Co-SAs/NPs@NC-850	557.3[a]	763.1
Co-SAs/NPs@NC-950	1403.8[a]	**1922.1**

[a] Gas production rate based on Co in the initial 1 hour.

In Line 59, we added "Indeed, many precious metal catalysts have been developed for formic acid dehydrogenation, with palladium-based catalysts, for example, exhibiting superior activity 50-200 times higher than low-cost metal catalysts.10-12 However, if the cost of the active metal is taken into account, e.g. palladium is >1000 times more expensive than cobalt, the search for highly active and stable non-noble

metal heterogeneous catalysts continues to attract the interest of many researchers in academia and industry. 13-15."

Question 2: The authors claim in their introduction that one of the great advantages of using such materials, instead of the already known and industrially used materials, is the cost reduction due to the fact that they are not based on noble metals. However, this type of catalyst is based on a hierarchically structured material with a zeolitic structure, which is subsequently pyrolysed with a relatively low yield. In this sense, this reviewer has two recurring questions, the first is could the authors determine the final yield in the synthesis of the catalyst, based on the final weight loss involved in the pyrolysis process. And the second is, have the authors carried out a market study to determine the price per kilogram of catalyst obtained? In this way, a fairer comparison can be made with the commercial catalyst and its potential can be highlighted.

Answer: MOF derived porous materials are currently a hotspot in catalyst research and have been widely used for photocatalysis, electrocatalysis, gas storage, rechargeable batteries and supercapacitors, so their yield is not a limiting factor.[4] Although the volatilization of Zn is unavoidable during conventional pyrolysis, the preparation is very simple and yields of more than 20% of the material can still be maintained.

For the first question, the final yield of the catalyst synthesis in our methods, calculated by dividing the pyrolyzed sample mass by the pre-pyrolysis, was 22.2 wt%. which was not low and comparable to the yields of current MOF-derived commercial catalytic products (19.5-34.0 wt%).[5] Considering that zinc can be recovered, the yield can be close to 50%.

For the second question, it is very difficult to do market research because in heterogeneous catalysis, the preparation of commercial catalysts is highly confidential, and the true price and yield of the catalysts are generally unknown. Indeed, many precious metal catalysts have been developed for formic acid dehydrogenation, which show excellent performance, with activities more than 50 times higher than that of low-cost metal catalysts. Nevertheless, considering the cost of the precious metals is more than 1,000 times that of cobalt (e.g., Co: $27,150/t, Pd: $901/t.oz), the search for highly

active and stable non-noble metal heterogeneous catalysts continues to attract the interest of many researchers in academia and industry (see table below for details).

Table. Comparison of the gas productivity per unit price of representative noble and non-noble metal catalysts for the dehydrogenation of formic acid.[1, 2]

Catalyst	TOF (h^{-1})	gas productivity per unit price ($L \cdot h^{-1} \cdot \$^{-1}$)
$[RuCl_2(PPh_3)_3$	2688	100.2
$[RuCl_2(C_6H_6)]_2$/DPPE	47970	1787.9
$[RuCl_2$(benzene)$]_2$/meso-P4	4580	170.7
$[(PNNNP^2)RuH_2(CO)]$	7300	272.1
$[(Cp^*Ir)_2(THBPM)Cl_2]Cl_2$	228000	334.7
[Cp*Ir(L41)Cl]Cl	487500	715.6
[Cp*Ir(pyrimidyl imidazoline)$H_2O]SO_4$	322000	472.6
Pd/N-MSC-30	8414	133.3
Pd@CN900K	14400	228.1
Co-N-C(SACs)	319.2[a]	884.0
Co-SAs/NPs@NC-750	257.7[a]	352.9
Co-SAs/NPs@NC-850	557.3[a]	763.1
Co-SAs/NPs@NC-950	1403.8[a]	**1922.1**

[a] Gas production rate based on Co in the initial 1 hour.

Question 3: There is some discrepancy in the process of catalyst synthesis. In the supporting info, the authors say that the catalysts have been pyrolysed in an inert atmosphere (Argon), however, in the discussion of results the authors say that the pyrolysis atmosphere is a reducing atmosphere (6%H_2 Ar balance), Line 110. If this is the case, how can the catalyst be reduced in an inert atmosphere during pyrolysis?

Answer: The Co-SAs/NPs@NC-950, Co-SAs/NPs@NC-850 and Co-SAs/NPs@NC-750 catalysts in the discussion of the results are different from the single-atom catalysts synthesized with previous literature methods in the supporting information. In this

study, we propose that modulation of the pyrolysis temperature under 6%H_2/Ar atmosphere allows the preparation of single atom catalysts (850&750) or single atom/nanoparticle composite catalysts (950).

The presence of atomically dispersed CoN_2C_2 units and nanoparticles in the Co-SAs/NPs@NC-950 catalysts was confirmed by HAADF-STEM and XAFS spectroscopy as well as DFT calculations. In the supporting information, to better compare with Co-N-C (SAC) containing the same CoN_2C_2 units, we refer to previous methods for the synthesis of catalysts by gradient pyrolysis up to 1000 ℃ in an argon atomosphere.[3] We prepared Co-N-C (SAC) mainly for comparative studies of promotion of CoN_2C_2 by nanoparticles.

To study the effect of H_2 pyrolysis conditions on potential catalytic materials, we did VTXRD, see below. As can be seen from Figure S4, the ZIF structure remained stable when the temperature is lower than 550 ℃, and as the temperature is further increased to 650, the ZIF structure started to collapse. When the temperature was increased to 750 and 850 ℃, amorphous carbon appeared, but no cobalt related signals appeared, indicating that cobalt was still atomically dispersed. Further increasing the temperature to 950 °C, the characteristic peaks of Co nanoparticles and graphitic carbon appeared, indicating that graphite-like carbon-encapsulated nanoparticle are formed on the catalyst. Moreover, we found that as the pyrolysis temperature increased, the single-atom catalysts (850&750) changed into single atom/nanoparticle composite catalysts (950). H_2/Ar reducing atmosphere promoted the transformation of some isolated metal atoms to nanoparticles based on variable temperature powder X-ray diffractometry (VTXRD).[6]

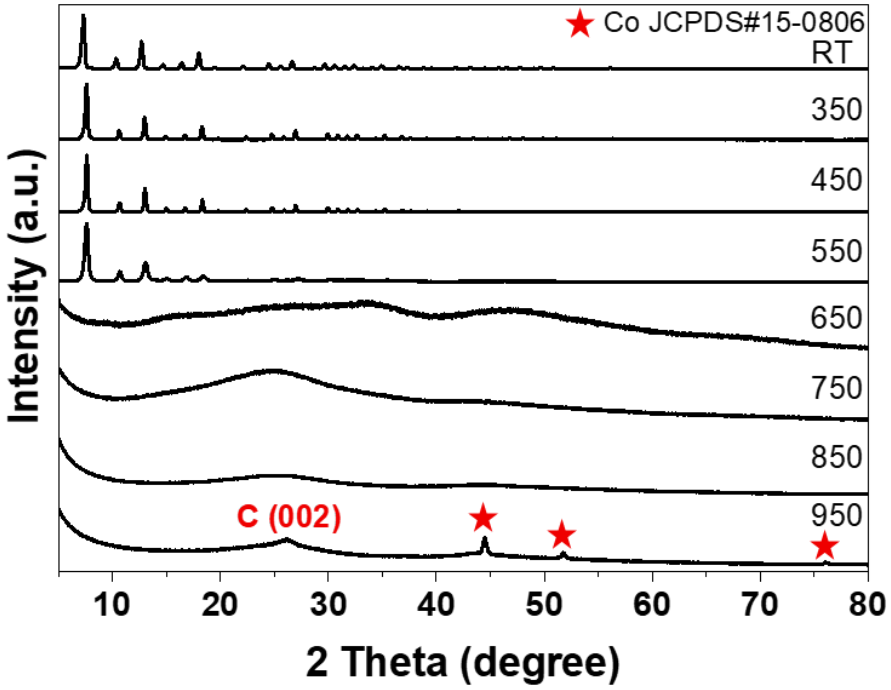

Figure S4. VTXRD spectra of cobalt-doped ZIF with pyrolysis temperatures ranging from room temperature to 950 ℃.

In Line 115, we added " Specific experimental observations at some key steps in the synthesis process are detailed in Figures S1 to S3. Variable temperature powder X-ray diffraction (VTXRD) was performed to monitor the catalyst evolution. After the pyrolysis temperature reached 650 °C, the XRD patterns changed significantly due to the collapse of the ordered crystal structure of ZIFs (Fig. S4).39 As the temperature increases further, XRD patterns of Co-SAs/NPs@NC-850 and Co-SAs/NPs@NC-750 revealed two broad peaks at 20-30° and 40-50°, representing the amorphous carbon peaks (Fig. S5).40 Notably, three characteristic peaks at 44.2°, 51.5°, and 75.8°, belonging to metallic cobalt (JCPDS #15-0806) and the peak at 26.2° belonging to graphitic carbon (JCPDS #41-1487) were observed only in the XRD spectra of the Co-SAs/NPs@NC-950, suggesting that graphite-like encapsulated cobalt nanoparticles appeared on the catalyst. 41-44 Raman spectra shows that Co-SAs/NPs@NC-950 appeared to have stronger and narrower D and G peaks than the other samples, indicating a higher degree of graphitization (Fig. S6)."

In the supporting experimental information, we modified "1.2 Preparation of Co SAs catalyst and 1.3 Preparation of Co NPs catalyst" to "1.2 Preparation of control Co SAs catalyst with CoN_2C_2 units and 1.3 Preparation of control Co NPs catalysts".

Question 4: Furthermore, the samples seem to be pyrolysed at different temperatures, 750, 850 and 950ºC in the manuscript and 800, 900 and 1000ºC in the supporting information. Please clarify this error and describe the process accordingly.

Answer: The catalysts prepared in the discussion of the results and in the supporting information are different, so different pyrolysis conditions are mentioned. We propose that modulation of the pyrolysis temperature under 6%H_2/Ar atmosphere allows the preparation of single atom catalysts (850&750) or single atom/nanoparticle composite catalysts (950), which can be confirmed by Variable temperature powder X-ray diffractometry (VTXRD). Characterization such as XAF and HAADF confirmed the single-atom unit as CoN_2C_2 in Co-SAs/NPs@NC-950, interestingly in agreement with previous studies. Therefore, in the supporting information, in order to better compare with Co-N-C (SAC) containing CoN_2C_2 units, we refer to previous methods to synthesize control catalysts by gradient pyrolysis up to 1000 ℃ in an argon atomosphere.[3] In the manuscript, the samples were pyrolysed at different temperatures (750 °C, 850 and 950) for comparing Co-SAs/NPs@NC-750, Co-SAs/NPs@NC-850 and Co-SAs/NPs@NC-950, respectively.

In Line 495, we modified "For the synthesis of Co-SAs/NPs@NC-950, the dried powder of CoZn-ZIF was pyrolyzed at 950 °C for 1 h with a ramping rate of 5 °C min-1 under 6% H2 + 94% Ar flow. The sample was then cooled to room temperature to obtain Co-SAs/NPs@NC-950. For Co-SAs/NPs@NC-850 or Co-SAs/NPs@NC-750, the pyrolysis temperatures were changed to 850 and 750 °C, respectively."

Question 5: The XRD of the presented catalysts have a very high noise-to-signal ratio, which makes it difficult to assign cobalt metal peaks to an amorphous carbon peak. The authors should repeat these XRDs with a higher step number to increase their resolution.

Answer: Following the suggestion of the reviewer, finer XRD measurements were reperformed, and the results were updated in Fig S5, with specific parameter changes as follows: the time/steps and steps were set to 0.2s and 18300, respectively. It allows to better distinguish the cobalt metal peaks from the amorphous carbon peaks. XRD patterns of Co-SAs/NPs@NC-850 and Co-SAs/NPs@NC-750 reveal two broad peaks at 20-30° and 40-50°, representing the amorphous carbon peaks (Fig. S5).[7] Three characteristic peaks with 2θ values located at 44.2°, 51.5°, and 75.8° are observed only in the XRD patterns of Co-SAs/NPs@NC-950, attributed to diffraction from the (111), (200), and (220) crystal planes of metallic cobalt (JCPDS #15-0806), suggesting the formation of Co nanoparticles.[8, 9] In addition, we found that the amorphous tendency of carbon gradually disappears with increasing temperature, and the characteristic peaks of C (002) and Co nanoparticles appear at 950 °C[10-12], and the reduction of H_2 on the surface causes some single atoms to agglomerate also changes the periodicity of the carriers, in agreement with the VTXRD results. In addition, combined with our theoretical calculations, we believe that in addition to the promotion of single atom by nanoparticles, graphitized carbon strengthens the electron transfer between monoatoms and nanoparticles due to the low resistance, which strengthens the active.[13]

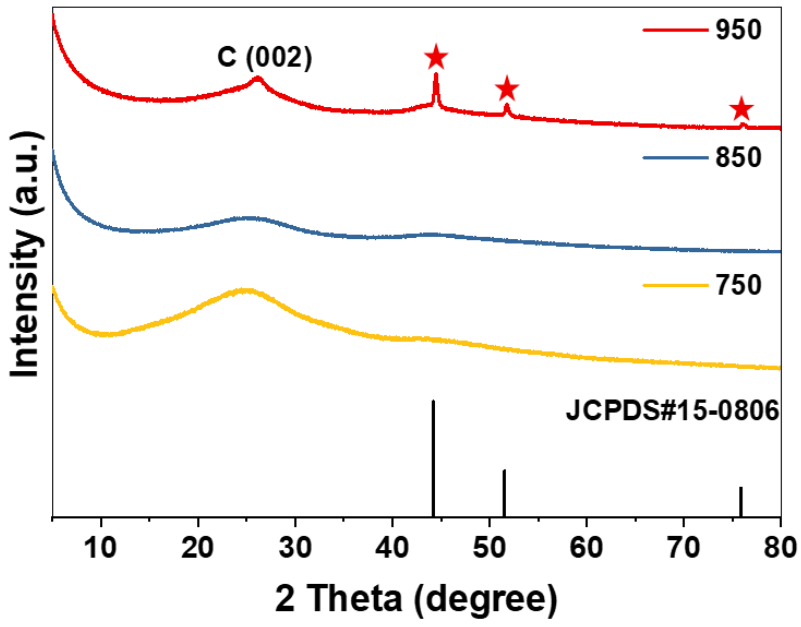

Figure S5. XRD spectra of Co-SAs/NPs@NC-950, Co-SAs/NPs@NC-850 and Co-SAs/NPs@NC-

750.

In ***Line 115, we modified "Specific experimental observations at some key steps in the synthesis process are detailed in Figures S1 to S3. Variable temperature powder X-ray diffraction (VTXRD) was performed to monitor the catalyst evolution. After the pyrolysis temperature reached 650 °C, the XRD patterns changed significantly due to the collapse of the ordered crystal structure of ZIFs (Fig. S4).39 As the temperature increases further, XRD patterns of Co-SAs/NPs@NC-850 and Co-SAs/NPs@NC-750 revealed two broad peaks at 20-30° and 40-50°, representing the amorphous carbon peaks (Fig. S5).40 Notably, three characteristic peaks at 44.2°, 51.5°, and 75.8°, belonging to metallic cobalt (JCPDS #15-0806) and the peak at 26.2° belonging to graphitic carbon (JCPDS #41-1487) were observed only in the XRD spectra of the Co-SAs/NPs@NC-950, suggesting that graphite-like encapsulated cobalt nanoparticles appeared on the catalyst. 41-44 Raman spectra shows that Co-SAs/NPs@NC-950 appeared to have stronger and narrower D and G peaks than the other samples, indicating a higher degree of graphitization (Fig. S6)."***

Question 6: The authors should add the cobalt particle size distributions found for the catalysts to the manuscript. It seems that, with increasing pyrolysis temperature, these distributions become wider.

Answer: According to your suggestion, we have added the cobalt particle size distribution of the catalyst to the manuscript and the nanoparticles appeared only when the pyrolysis temperature rose to 950 °C. The particle size distribution is not studied for single atom catalysts, and only in the case of nanoparticle catalysts, the TEM images show a histogram of the size distribution.[14] In the manuscript, Co-SAs/NPs@NC-850 and Co-SAs/NPs@NC-750 are both single-atom catalysts, and we provided the particle size distribution of Co-SAs/NPs@NC-950 in Figure S8 in the revised Supporting information, which shows that the average particle size of the nanoparticles is 7.48 ± 1.74 nm.

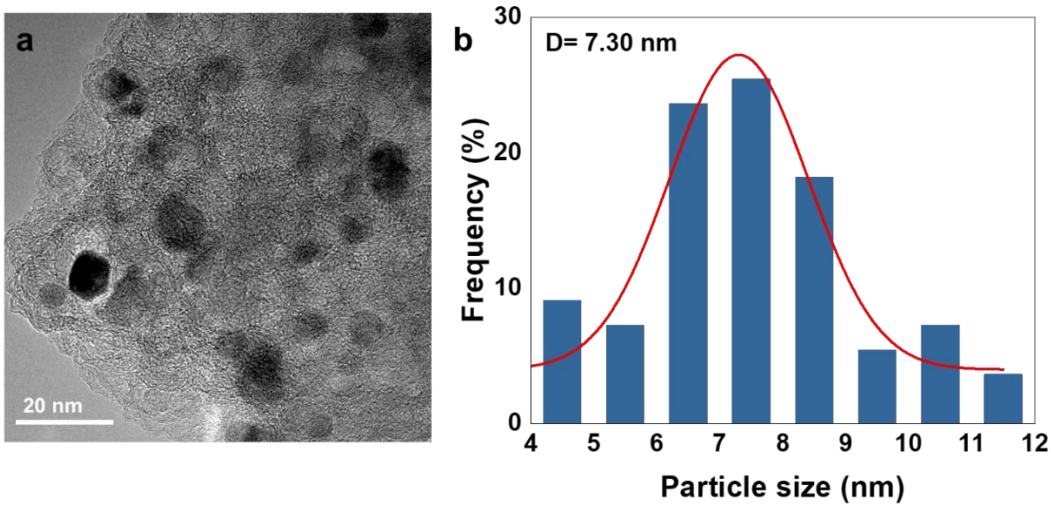

Figure S8. a TEM image and **b** the corresponding particle-size distribution histogram of Co-SAs/NPs@NC-950.

In ***Line 144 we added "Notably, transmission electron microscopy (TEM) proves the presence of distinct cobalt nanoparticles (NPs) with an average size of 7.5 ± 1.7 nm only in Co-SAs/NPs@NC-950 (Fig. 1b and Fig. S8)."***

Question 7: **Elemental analysis of the samples should be done to evaluate the percentage of nitrogen, oxygen, carbon and hydrogen in the samples.**

Answer: According to your suggestion, we supplemented the elemental analysis of the Co-SAs/NPs@NC-950, Co-SAs/NPs@NC-850 and Co-SAs/NPs@NC-750, see Table S3 below. Elemental analysis (EA) shows that the proportion of N decreased and the proportion of C increased with increasing pyrolysis temperature, in agreement with the available literature.[15] The high levels of O may be related to adsorption of O_2 due to exposure to air.

Table S3. Elemental analysis of the Co-SAs/NPs@NC-950, Co-SAs/NPs@NC-850 and Co-SAs/NPs@NC-750.

Catalysts	N/%	C/%	H/%	O/%
Co-SAs/NPs@NC-750	16.53	48.47	3.01	21.75
Co-SAs/NPs@NC-850	10.42	64.71	2.43	24.14

Co-SAs/NPs@NC-950	3.36	67.79	3.00	24.61

In ***Line 139, we added "Elemental analysis (EA) shows that as the pyrolysis temperature increases, the percentage of N decreases, the percentage of C increases, and the high content of O may be related to adsorption of O_2 due to exposure to air. (Table S3)."***

Question 8: It seems contradictory, that the authors show particles measured in HAADF-STEM, for all three catalysts, Figure 1c and Figure s6, with sizes clearly below 500 pm, yet they are able to see a peak associated with metallic cobalt by XRD. How is this possible?

Answer: It should be noted that we did not see nanoparticles in the HADDF for Co-SAs/NPs@NC-850 and Co-SAs/NPs@NC-750. We propose that modulation of the pyrolysis temperature under 6%H_2/Ar atmosphere allows the preparation of single atom catalysts (850&750) or single atom/ nanoparticle composite catalysts (950). For Co-SAs/NPs@NC-950, the presence of cobalt nanoparticles was observed in HRTEM (Figure 1b), but our original HAADF-STEM was primarily intended to provide evidence for single atoms, so we did not select regions with nanoparticles. To ameliorate this problem, we re-provided the HAADF-STEM images and the results were updated in Figure 1c, demonstrating the simultaneous existence of single atoms and nanoparticles. In our study, the peaks of metallic cobalt are only observed in Co-SAs/NPs@NC-950 in the XRD pattern, which is consistent with 7-8 nm Co nanoparticles in HRTEM and HAADF-STEM, along with the presence of Co-Co metallic bonds in EXAFs. For Co-SAs/NPs@NC-850 and SAs/NPs@NC-750, only atomically dispersed cobalt is observed in the HAADF (Figure S9), which is consistent with the absence of metallic cobalt peaks observed in the XRD, as well as the absence of Co-Co bands in the EXAFs.

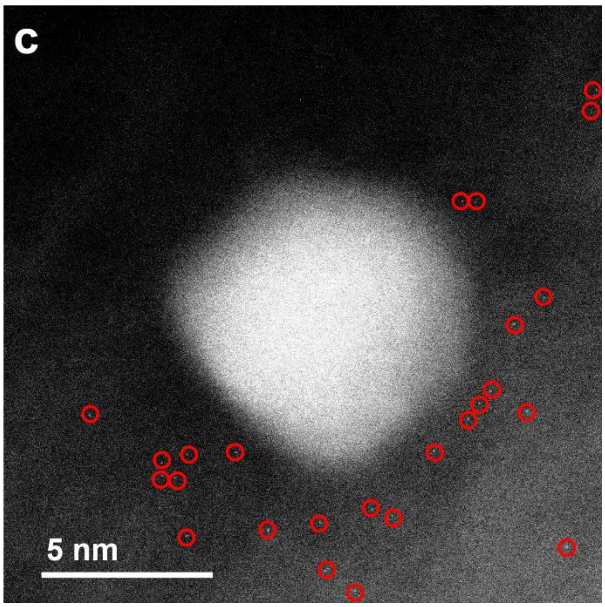

Figure 1c. AC-HAADF-STEM image of Co-SAs/NPs@NC-950, the Co single atoms are marked with red circles.

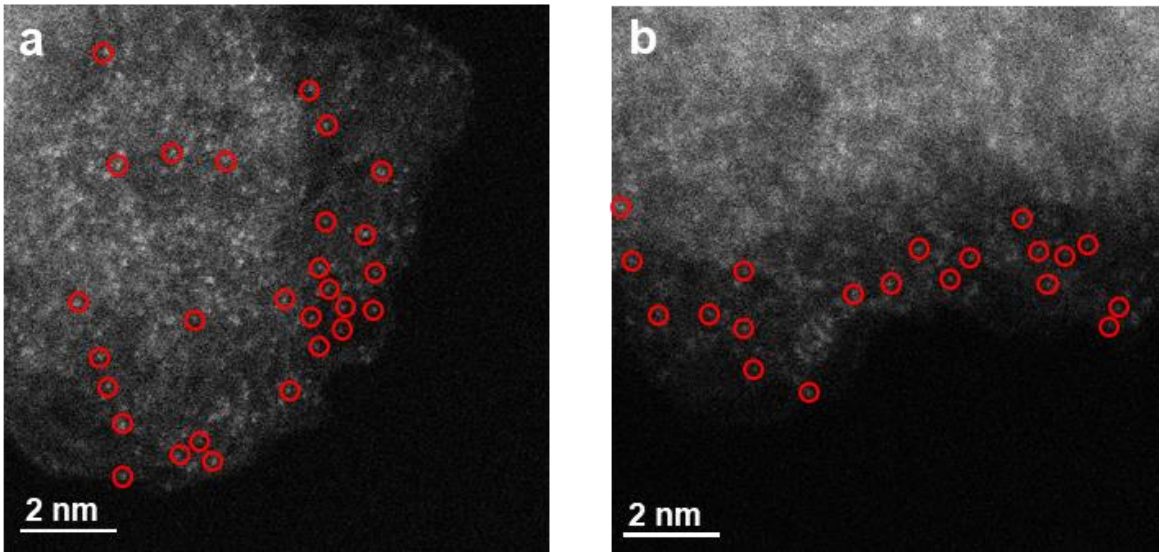

Figure S9. The HAADF-STEM image of **a** Co-SAs/NPs@NC-850 and **b** Co-SAs/NPs@NC-750 with a resolution of 2 nm. The Co single atoms are marked with red circles.

In ***Line 150, we modified "Further, aberration-corrected high-angle annular dark-field scanning transmission electron microscopy (AC-HAADF-STEM) reveals Co NPs were surrounded by cobalt in Co-SAs/NPs@NC-950 (Fig. 1c). However, only atomically dispersed cobalt atoms were observed on the support in the other two samples (Fig. S9)."***

Question 9: It is strange that the 002 peak for amorphous carbon in the XRD is more crystalline for the sample pyrolysed at 850 than for the sample pyrolysed at 950C. This would indicate that the sample pyrolysed at 850C is more graphitic than the sample pyrolysed at the higher temperature? The authors should calculate the R and Lc values, following the approach of Alexander et al. for all catalysts (L. E. Alexander and E. C. Sommer, J. Phys. Chem., 1956, 60, 1646–1649).

Answer: The finer XRD measurements were reperformed, and the results were updated in Fig S5, with specific parameter changes as follows: the time/steps and steps were set to 0.2s and 18300, respectively. In the XRD spectra of Co-SAs/NPs@NC-950, the 2θ peak with a value of 26.2° (JCPDS #41-1487) belongs to graphitic carbon, which is much stronger than the broad peak of Co-SAs/NPs@NC-850 and Co-SAs/NPs@NC-750 at 24° attributed to amorphous carbon.[7, 10-12] This proves that the sample pyrolyzed at 950℃ is more graphitized than other samples pyrolyzed at the lower temperature.

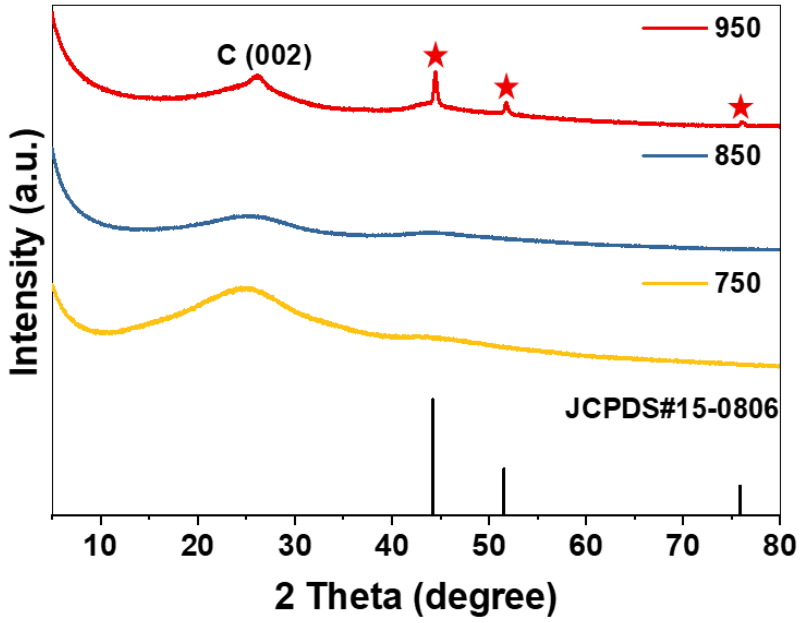

Figure S5. XRD spectra of Co-SAs/NPs@NC-950, Co-SAs/NPs@NC-850 and Co-SAs/NPs@NC-750.

Moreover, we have calculated the empirical parameter, R and stacking height, Lc values following the approach of Alexander et al. and Liu et al. for all catalysts as shown in the following table.[16, 17] The three samples have similar R-values, indicating

a comparable number of monolayer-aligned carbon flakes. However, Co-SAs/NPs@NC-950 had the larger Lc value, indicating the presence of graphitic carbon the graphitization.

Table. The R and Lc values of Co-SAs/NPs@NC-950, Co-SAs/NPs@NC-850 and Co-SAs/NPs@NC-750.

Catalysts	R	L_c/nm
Co-SAs/NPs@NC-750	1.87	0.56
Co-SAs/NPs@NC-850	1.54	0.58
Co-SAs/NPs@NC-950	1.71	4.73

Question 10: This author does not entirely agree with this statement, "The similar cobalt content in the three catalysts suggests that the coordination structure of the active site rather than the metal content is responsible for the differences in performance, as discussed below" as it has been extensively studied and published for this reaction, that not only the metal loading is responsible, but also the particle size of the metal. It has been found that the reaction is structure-sensitive. (Chemical Engineering Journal 420 (2021) 127641, J. Catal. 352 (2017) 371–381, ACS Appl. Mater. Interfaces 9 (2017) 24678–24687, ChemistrySelect 1 (2016) 1879–1886).

Answer: It is not true that the sentence describing only the ligand structure of the active site is responsible for the difference in performance. We reviewed these papers and they all mention the relationship between particle size and activity, so the particle size of the active metal, the exposed crystal surface, and the coordination environment all affect the activity.[18, 19] In order to better investigate the structure-activity relationship of Co-based catalysts, we previously conducted a coordination effect study and found that Co-N-C with CoN_2 by gradient pyrolysis up to 1000 ℃ in an argon atmosphere has the best activity compared to CoN_3 and CoN_4.[3] Interestingly, the single atom units in Co-SAs/NPs@NC-850 and Co-SAs/NPs@NC-750 in our study are CoN_3 and CoN_4, respectively. According to our investigations, the coexistence of nanoparticles and

single atom Co_2N_2 promotes formic acid dehydrogenation. Therefore, in addition to modulating the structure of the active site, modulation of nanoparticles and single-atom interactions could likewise increase activity at similar cobalt content.

In ***Line 142, we modified the text to " At certain cobalt contents, nanoparticles and isolated co-atoms coexist, which leads to a considerable increase in catalyst activity, as explained below."***

Question 11: This author disagrees with this statement, "All these results indicate that atomically dispersed Co sites and N-doped graphite-encapsulated nanoparticles are successfully anchored on NC carriers in Co-SAs/NPs@NC-950, whereas only single metal sites are present in the other samples", for many reasons. First of all, there is no evidence of graphite in the samples, since the XRD of all samples show broad, undefined peaks characteristic of amorphous carbons and not graphite. Secondly, the sample calcined at a higher temperature shows a lower proportion of nitrogen groups, as the authors claim in the paragraph below. That is why the number of NC carriers in this sample should be lower than in the others. And consequently, the anchoring of the weaker active phase, results in greater sintering of the cobalt particles.

Answer: We agree with you that there is no "standard" crystalline graphite in the described materials. Instead, it is N-doped graphite-like carbon-encapsulated structures, as evidenced by the strong and narrow D and G peaks in the complementary Raman spectra and the graphite streaks in the HRTEM of Co-SAs/NPs@NC-950 (Figure S6 and Figure 1b). We supplemented the Raman spectra with results showing that Co-SAs/NPs@NC-950 appeared to have stronger and narrower D and G peaks than the other samples, indicating a higher degree of graphitization (Figure S5). In transmission electron microscopy, Co-SAs/NPs@NC-950 exists lattice streaks with a spacing of 0.361 nm, attributed to graphitic carbon (002), which is consistent with the graphitic carbon peak observed at 26.2° by supplemental XRD (JCPDS #41-1487). The above evidence suggests that the formation of graphite-like carbon.

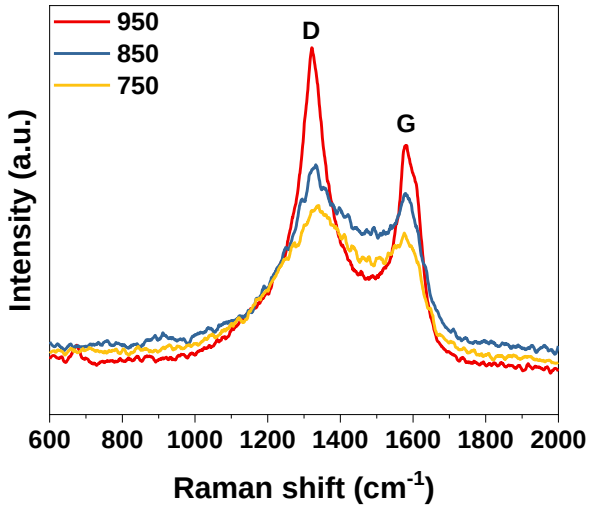

Figure S6. Raman spectra of Co-SAs/NPs@NC-950, Co-SAs/NPs@NC-850 and Co-SAs/NPs@NC-750.

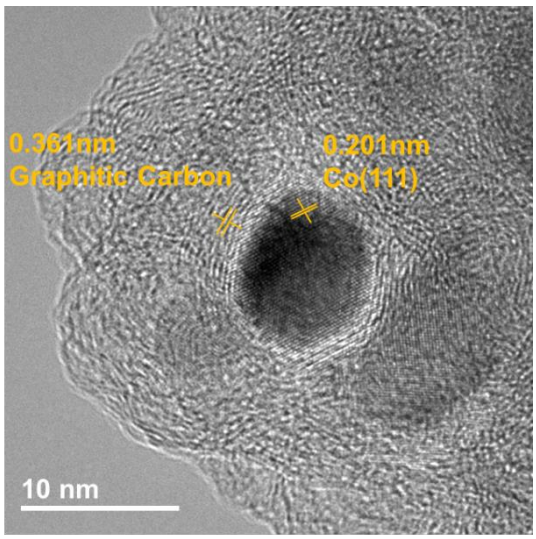

Figure 1b. TEM image of Co-SAs/NPs@NC-950.

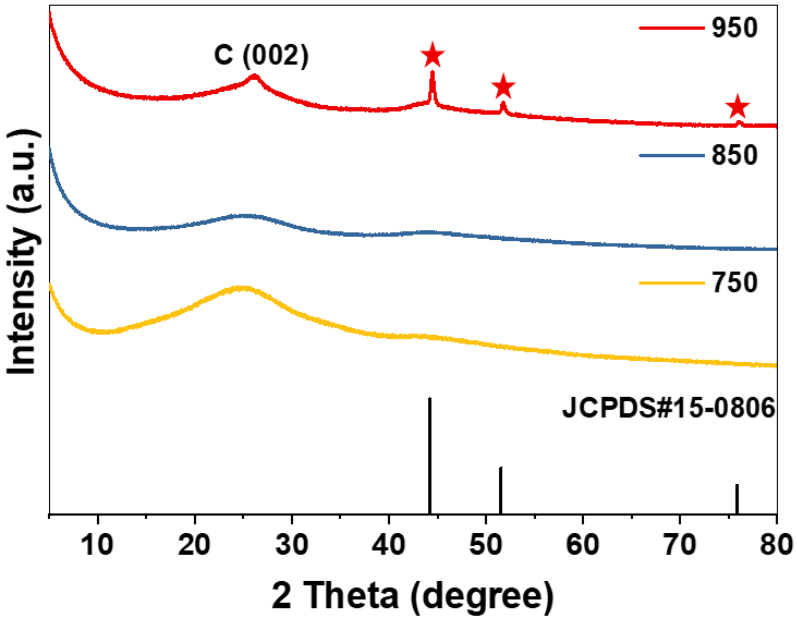

Figure S5. XRD spectra of Co-SAs/NPs@NC-950, Co-SAs/NPs@NC-850 and Co-SAs/NPs@NC-750.

As for your second point, we recognize that it supports our conclusions. Indeed, the proportion of nitrogen groups is lower in samples calcined at higher temperatures, so the number of NC carriers in Co-SAs/NPs@NC-950 should be lower than in other samples, resulting in anchoring of the weaker reactive phases leading to more cobalt particle sintering.

In ***Line 127, we added the following text "Raman spectra shows that Co-SAs/NPs@NC-950 appeared to have stronger and narrower D and G peaks than the other samples, indicating a higher degree of graphitization (Fig. S6)."***

In ***Line 148, 157, and 456, we modified "N-doped graphite" to "N-doped graphite-like carbon."***

In ***Line 176, we added "The lower proportion of nitrogen atoms in the samples pyrolyzed at higher temperatures means that the number of NC carriers in Co-SAs/NPs@NC-950 should be lower than in other samples. This leads to a stronger sintering of the cobalt particles."***

Question 12: What is the effect of zinc on the stabilization of cobalt particle size? According to the synthesis procedure, the same amount of zinc nitrate as

methylimidazole is added at the beginning of the synthesis. Are there traces of zinc in the pyrolyzed catalyst? The effect of possible zinc remaining in the catalyst after pyrolysis must be added to the discussion of the results. At the same time, the study of the loading of the different metals of the catalyst by ICP is required for the discussion of the results.

Answer: We compared the TEM images of the catalysts pyrolyzed with different precursors (CoZn-ZIF and Co-ZIF) as follows: Atomically dispersed or small nanoparticles of cobalt (7.5 ± 1.7 nm) are observed in the Co-N-C obtained when CoZn-ZIF was used as the pyrolysis precursor (Figures a and b). When the Co-ZIF was used as the pyrolysis precursor, only ellipsoidal morphology NPs were found on the carbon carriers with a diameter of about 10 nm (Figure c).[3] The doping of Zn improves the dispersion and porosity of the metal catalysts by volatilization of Zn at elevated temperatures, thus increasing the activity and stability of the catalysts.[20]

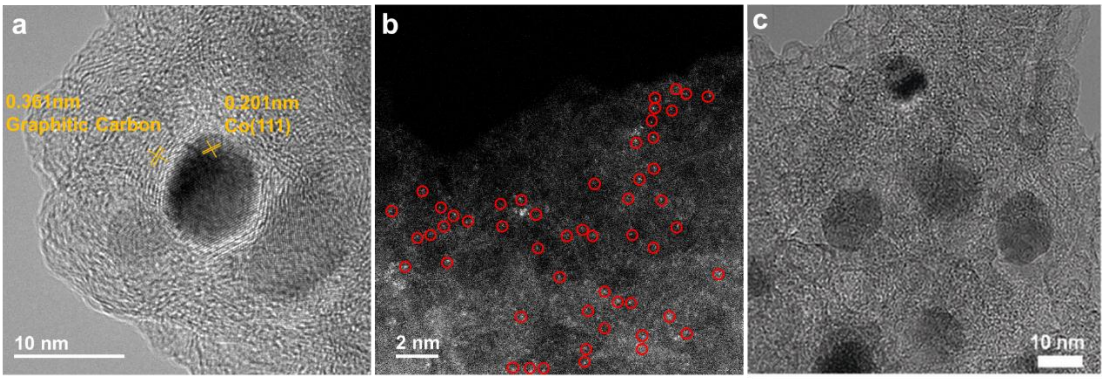

Figure a TEM image. **b** AC-HAADF-STEM image of the catalysts pyrolyzed with CoZn-ZIF, the Co single atoms are marked with red circles. **C** TEM image of the catalyst pyrolyzed with Co-ZIF.

The loadings of cobalt and zinc in the catalysts were investigated by AAS, and the three materials possessed similar cobalt contents, while the zinc contents of Co-SAs/NPs@NC-950, Co-SAs/NPs@NC-850, and Co-SAs/NPs@NC-750 gradually increased. During pyrolysis, Zn nodes are reduced and volatilized (Zn, boiling point = 907 °C), which promotes the formation of porous structures.[21, 22] Moreover, with increasing pyrolysis temperature, Co-SAs/NPs@NC-950 possesses a larger specific surface area than Co-SAs/NPs@NC-850 and Co-SAs/NPs@NC-750, which is

attributed to more zinc evaporation during pyrolysis. In addition, we supplemented Zn-ZIF-8 and Zn-N-C obtained by pyrolyzing Zn-ZIF-8. The resulting materials were no active for formic acid dehydrogenation, suggesting that Zn is not an active center and the effect on the activity can be ignored (Figure 3a). In summary, we assume the presence of Zn positively affects the size regulation of Co nanoparticles, but does not affect the activity of the cobalt.

Table S2. Cobalt and zinc content of the Co-SAs/NPs@NC-950, Co-SAs/NPs@NC-850 and Co-SAs/NPs@NC-750 tested by AAS.

Catalysts	Co/%	Zn/%
Co-SAs/NPs@NC-750	2.73	6.37
Co-SAs/NPs@NC-850	2.74	2.68
Co-SAs/NPs@NC-950	2.69	/

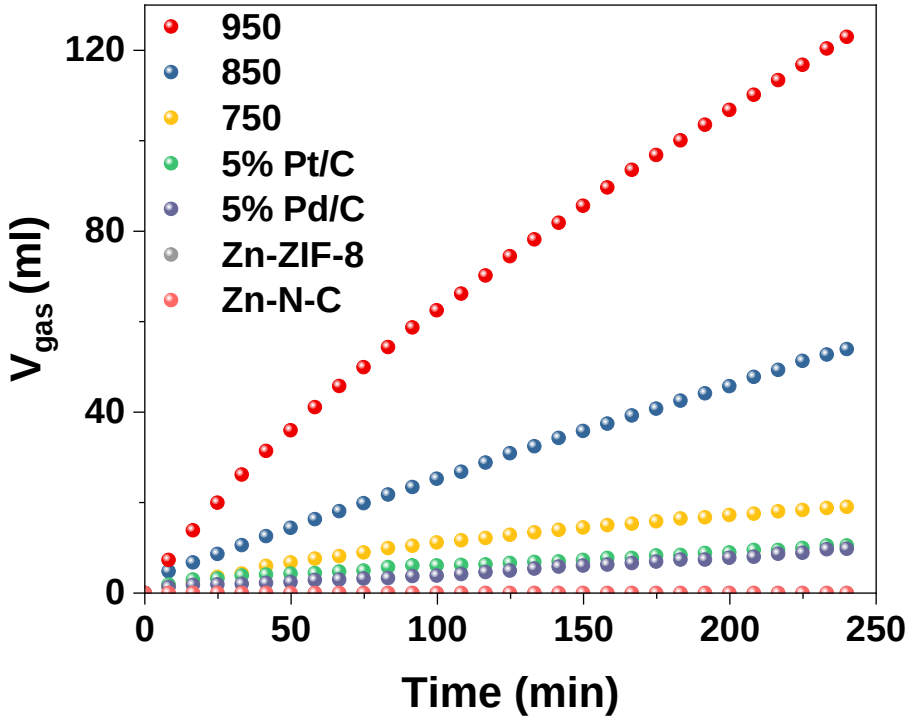

Figure 3a Plot of volume of produced gas versus time for the dehydrogenation of FA applying different catalysts. Reaction conditions: FA (10 mmol, 377 μL), catalyst (30 mg), PC (6 mL), T_{set}: 110 °C, T_{actual}: 98 °C, 4h.

In Line 135, we added "The zinc content of Co-SAs/NPs@NC-950, Co-SAs/NPs@NC-850, and Co-SAs/NPs@NC-750 increased progressively, which was attributed to the increased reduction and volatilization of Zn nodes with increasing pyrolysis temperatures (Zn, boiling point = 907 °C)."

In Line 249, we added "Moreover, the Zn-ZIF-8 and Zn-N-C were no active for formic acid dehydrogenation, suggesting that Zn is not an active center and the effect on the activity can be ignored."

Question 13: The general XPS spectrum and the zinc and oxygen spectrum should be added to the manuscript for discussion, as well as a table with the atomic percentages for each species.

Answer: According to your suggestion, general XPS spectra, as well as zinc and oxygen spectra, are included in the manuscript for discussion, and the atomic percentages of each substance are listed in Table S4. X-ray photoelectron spectroscopy (XPS) survey spectra of the three catalysts showed the presence of the elements Co, N, C, and O, but zinc is present only in Co-SAs/NPs@NC-850 and Co-SAs/NPs@NC-750 (Figure S10). As the pyrolysis temperature increases, the total N content decreases because N species are unstable and decompose into NH_3 and NO_x gases at higher temperatures (Table S4). The O 1 s spectrum shows two peaks for C=O (531.6 eV) and C-O (533.5 eV), respectively (Fig. S12). The Zn 2p spectra reveals that the Zn $2p^{1/2}$ peak located at 1044.6 eV and the Zn $2p^{3/2}$ peak located at 1021.5 eV indicating the presence of elemental Zn mainly in the form of Zn^{2+} (Fig. S13)

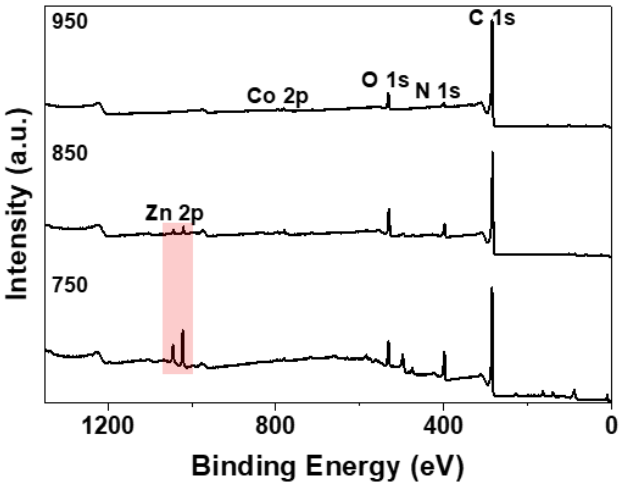

Figure S10. XPS survey scanning of Co-SAs/NPs@NC-950, Co-SAs/NPs@NC-850 and Co-SAs/NPs@NC-750.

Table S4. The atomic percentages of each substance of the Co-SAs/NPs@NC-950, Co-SAs/NPs@NC-850 and Co-SAs/NPs@NC-750.

Catalysts	C/%	N/%	O/%	Co/%	Zn/%
Co-SAs/NPs@NC-750	73.23	13.78	7.89	0.47	4.62
Co-SAs/NPs@NC-850	80.46	8.57	9.74	0.66	0.56
Co-SAs/NPs@NC-950	87.73	4.02	7.80	0.46	0

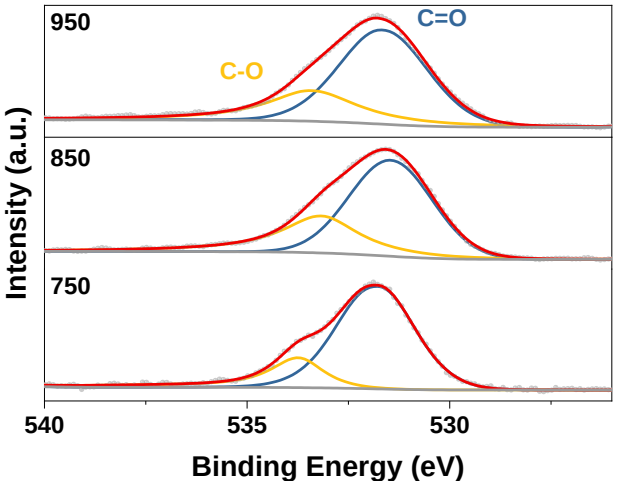

Figure S12. XPS spectra of O 1s of Co-SAs/NPs@NC-950, Co-SAs/NPs@NC-850 and Co-

SAs/NPs@NC-750.

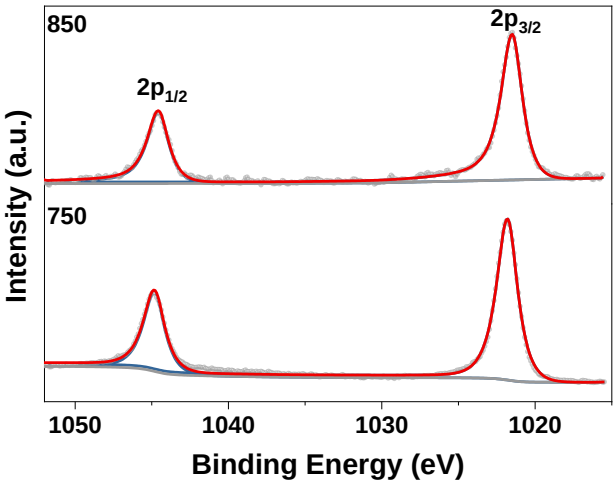

Figure S14. XPS spectra of Zn 2p of Co-SAs/NPs@NC-850 and Co-SAs/NPs@NC-750.

In Line 169, we added "X-ray photoelectron spectroscopy (XPS) survey spectra of the three catalysts showed the presence of the elements Co, N, C, and O, but zinc was present only in Co-SAs/NPs@NC-850 and Co-SAs/NPs@NC-750 (Fig. S10)."

In Line 179, we added "The O 1 s spectrum shows two peaks for C=O (531.6 eV) and C-O (533.5 eV), respectively (Fig. S13)."

In Line 190, we added "The Zn 2p spectra revealed that this element is mainly present in the form of Zn^2 (Fig. S14)."

Question 14: The XPS spectra of the manuscript should be generally reviewed and corrected. The assignment and deconvolution of the cobalt XPS spectrum should be reviewed. The assignment for the Co-N species, (781.6 eV from NIST), appears to be shifted to lower binding energy for the 750 and 850 C samples. Likewise, the width of the peak assigned to graphitic N in the nitrogen spectrum is much higher than that of the rest of the peaks.

Answer: According to your suggestion, we reviewed and corrected the cobalt and nitrogen XPS spectrum. Indeed, for the 750 and 850 °C samples, the Co-N peak shifted to a lower binding energy compared to the assignment for the Co-N species (781.6 eV from NIST), indicating an elevated electron density for Co species, which is in

agreement with other literature works (Figure 2b).[25-27] In the nitrogen spectrum, the width of the N-doped graphite peak is much higher than that of the other peaks because the original half peak width was not controlled, and for better comparison, we reassigned the graphite N peak at 402.3 eV, and the results are updated in Figure 2a.[28]

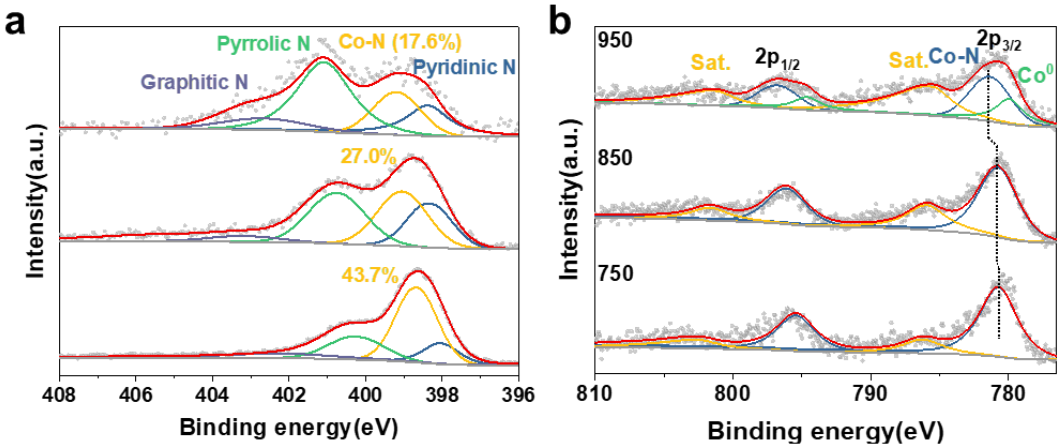

Figure 2a N 1s and **b** Co 2p spectra of Co-SAs/NPs@NC-T.

Question 15: Authors claim that "The observed formic acid dehydrogenation activities under the same conditions were in the order of Co-SAs/NPs@NC-950 > Co SAs > Co NPs, showing that the atomically dispersed CoN_2C_2 sites are more active than NPs. Could these differences be attributed to the presence of zinc in the samples?

Answer: These differences are not related to the presence of zinc in the samples for the following reasons. With the help of zinc evaporation, metal ions are dispersed at the atomic level on N-doped porous carbon. Co-SAs/NPs@NC-950, Co SAs and Co NPs are obtained by pyrolysis at higher temperatures than the boiling point of zinc (907°C) and no zinc was detected in the resulting materials by AAS. Moreover, Zn-ZIF-8 and Zn-N-C samples obtained by pyrolyzing Zn-ZIF-8 were not active for formic acid dehydrogenation (Figure 3a), suggesting that Zn is not an active center for such reactions and does not affect the activity, as mentioned in our previous study.[3] The above results show that zinc has no effect on the reaction.

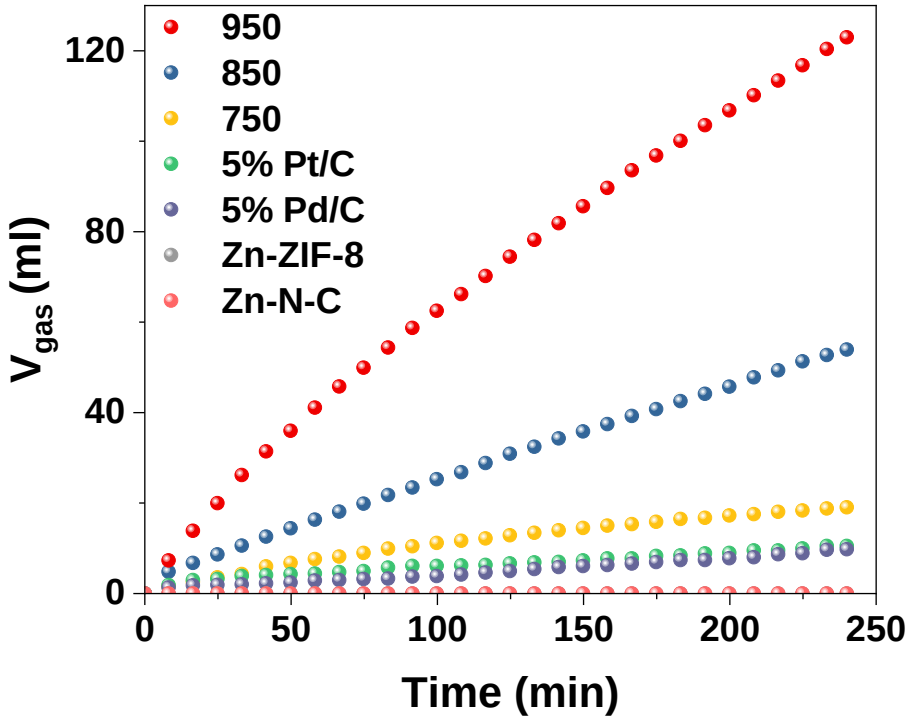

Figure 3a Plot of volume of produced gas versus time for the dehydrogenation of FA applying different catalysts. Reaction conditions: FA (10 mmol, 377 µL), catalyst (30 mg), PC (6 mL), T_{set}: 110 °C, T_{actual}: 98 °C, 4h.

Question 16: Equation S3 of supporting info is poorly described. To calculate the turnover frequency, TOF, the authors must calculate the number of moles of H_2, divide it by the number of total moles of Co, and the reaction time. The TOF values should be recalculated to compare with the literature.

Answer: Equation S3 of supporting information is not misrepresented. The current literature uses a standardized formula to calculate the catalyst TOF. We calculated the TOF in terms of H_2 moles and found a slight enhancement (1%) as the H_2/CO_2 produced in the reaction was 1.01. However, much of the literature is calculated in terms of moles of gas produced as the formic acid decomposition reaction rate is taken into account, and therefore we would like to retain the TOF algorithm in the revised manuscript. It should be the molar amounts of carbon dioxide and hydrogen, which are the main products, divided by the number of total moles of Co, and the reaction time.[3, 29, 30] We

added TOF values for comparison with the literature, as detailed in Table S12. The TOF value of our proposed Co-SAs/NPs@NC-950 was calculated to be 83 h^{-1}, which is higher than that of some noble metal catalysts (Table S12). Moreover, the calculation of TOF is based on the total cobalt content and does not distinguish between single atoms and nanoparticles. If the TOF is calculated using only single atoms, it should be higher than that of the Co-N-C (SACs) proposed in 2020, whose TOF was calculated as 357 h^{-1}. Thus, the presented Co-SAs/NPs@NC-950 shows excellent activity for formic acid dehydrogenation.

Table S12. Comparison of catalytic performance for FA dehydrogenation.

Catalyst	Other reactants	Temp.(°C)	TOF (h^{-1})	Selectivity (%)
$Ti_3C_2T_x$-250	H_2O	80	960	100
Co-N_4P SA sites	H_2O	80	589.5	≈100
Pd/Cvin. $ZnCl_2$	H_2O	50	76	100
Au–Pd/ED-MIL-101	H_2O+Sodium formate	90	57	100
$Co_{0.30}Au_{0.35}Pd_{0.35}$/C	No	25	80	100
Pd/N-CM (≈2.6 nm)	No	100	436	95.50
Co(1)/phen(7)/C	No	98	220	99.80
Co-N-C (SACs)	No	98	357	99.63
Co-SAs/NPs@NC-750	No	98	15	
Co-SAs/NPs@NC-850	No	98	46	
Co-SAs/NPs@NC-950	**No**	**98**	**83[a]**	

[a] The TOF was calculated based on the total content of single atoms and nanoparticles.

Question 17: Equation S6 is incorrectly calculated and if the selectivity has been calculated following this equation, it must be recalculated again. The selectivity

towards hydrogen should be Volume of hydrogen, divided by the volume of hydrogen, carbon monoxide and carbon dioxide.

Answer: The calculation of Equation S6 is reasonable.

$$HCOOH\ (l) \rightarrow H_2\ (g)+CO_2\ (g) \quad (S1)$$

$$HCOOH\ (l) \rightarrow H_2O\ (l)+CO\ (g) \quad (S2)$$

In general, FA decomposition can take place following the two processes shown in Equations S1 and S2. Due to the high coordination ability of CO, the formation of CO typically deactivates the catalyst, which is detrimental for direct fuel cell applications. Therefore, the dehydration pathway (Equation S2) should be avoided against the dehydrogenation pathway (Equation S1). Hence, the selectivity of the hydrogen production reaction from formic acid is important and not just the hydrogen selectivity. The current literature uses standardized formulas to calculate such selectivity.[3, 31] Hydrogen and carbon dioxide are the products in the main reaction, and one of the two is chosen for the calculation. We chose hydrogen as the representative amount of the main product.

Question 18: There are figures that on a scientific level do not contribute anything to the manuscript, such as figures S1, S2, S3, and S17. They could be removed from the supporting information, without compromising the essential information.

Answer: Here, we disagree with the reviewer. We believe these images are useful for scientists who want to perform similar experiments. The figures reflect the apparent changes in the samples during synthesis and before and after the reaction. We added Figures S1, S2, and S3 to facilitate the observation of changes in experimental phenomena at some key steps during synthesis, similarly mentioned in other literature.[32, 33] Figure S17 is presented to visualize the changes in the catalyst before and after the reaction.[3] We observed no apparent color change or aggregation of the catalyst, and the combination of XPS, HAADF, and EDS characterization proved the stability of the proposed catalysts.

In Line 115, we added "Specific experimental observations at some key steps in the synthesis process are detailed in Figures S1 to S3."

In Line 299, we added "No apparent color change or aggregation of the catalyst was observed before or after the reaction (Fig. S33)."

Response to Reviewer 2:

Reviewer 2's comments: The manuscript entitled Combination of Nanoparticles with Single-Metal Sites Synergistically Boosts Co-Catalyzed Formic Acid Dehydrogenation is a very interesting article as the authors claim that nanoparticles and single atoms act synergistically to facilitate the facile dehydrogenation of formic acid, more efficiently than many noble metal catalysts. The introduction of the manuscript is highly informative, places the work in context and justifies the importance of the project and the need to develop new catalyst technology and identify more stable and efficient systems. The work is meticulous and thorough across catalyst preparation, characterization and catalyst evaluation/comparison and post catalysis analysis and the results provide a significant advance to the area of catalyst development for hydrogen technologies and as such will be of interest to academic and industrial researchers in allied areas. Overall, the work has been conducted to a very high standard and could be suitable for publication in Nature Communications, if the other reviewers agree, as it reports a new concept in XXX (although synergy between supported SAs and NPs has been reported Adv. Mater. 2022, 34, 2200057, ACS Nano 2021, 15, 9, 14453–14464, Applied Catalysis B: Environmental 2023, 323, 122190) that could represent a significant advance in catalyst discovery for hydrogen storage, as such I recommend publication after addressing the following comments and conducting associated revisions.

Our response: We thank the referee for the comments and high praise. Based on your suggestions, we added VTXRD to reveal the catalyst evolution during pyrolysis process. Characterizations (HAADF-STEM, XRD, BET, XPS) of Co-SAs/NPs@NC-950-1h, Co-SAs/NPs@NC-950-0.5h and Co-SAs/NPs@NC-950-2h were done to clarify the effect of pyrolysis time on catalyst structure and activity. In addition, based on your suggestions, we have supplemented the hydrogen reaction kinetics and further discovered the activity-enhancing effect of single-atom and nanoparticle coexistence.

Question 1: Define PC at the earliest possible disclosure, presumably in the abstract where it should be described as the optimum solvent.

Answer: In Line 31, we modified the text to "The optimal material with atomically dispersed CoN2C2 units and encapsulated 7-8 nm nanoparticles achieved an excellent gas yield of 1403.8 mL·g-1·h-1 using propylene carbonate (PC) as solvent, with no activity loss after 5 cycles, which is 15 times higher than that of the commercial Pd/C."

Question 2: Page 6 ln 107- What happens if you change the Co:Zn ratio in the catalyst synthesis? At the very least the authors should defend their choice of the ratio, but it would be more informative to have some comparative data.

Answer: We supplemented the samples with different Co/Zn molar ratios for comparison of the effect of metal-element ratios on Co during preparation. Typically, the addition of Zn precursor was 30 mmol, and the cobalt precursor was added using 0.875, 1.75, 2.625, 3.5, 7, and 14 mmol, respectively (See Supplementary Information for details). As the cobalt content increases, it first exhibits a similar gas production rate and then decreases. The results showed that the catalyst reached the most excellent activity when 30 mmol $Zn(NO_3)_2$ and 3.5 mmol $Co(NO_3)_2$ were added. The above phenomenon is related to the difference in the existence form of cobalt at different contents, which is also proved by the subsequent kinetic experiments (see answer to question 10).

Table S6. Cobalt content and gas production rate of samples with different CoZn ratios.

$Zn(NO_3)_2$/mmol	$Co(NO_3)_2$/mmol	Co/%	Gas generation rate ($mL \cdot g_{Co}^{-1} \cdot h^{-1}$)
30	0.875	1.74	518.7
30	1.75	1.88	518.4
30	2.625	2.26	520.0
30	3.5	2.69	521.9
30	7.0	3.02	474.9
30	14.0	3.58	404.7

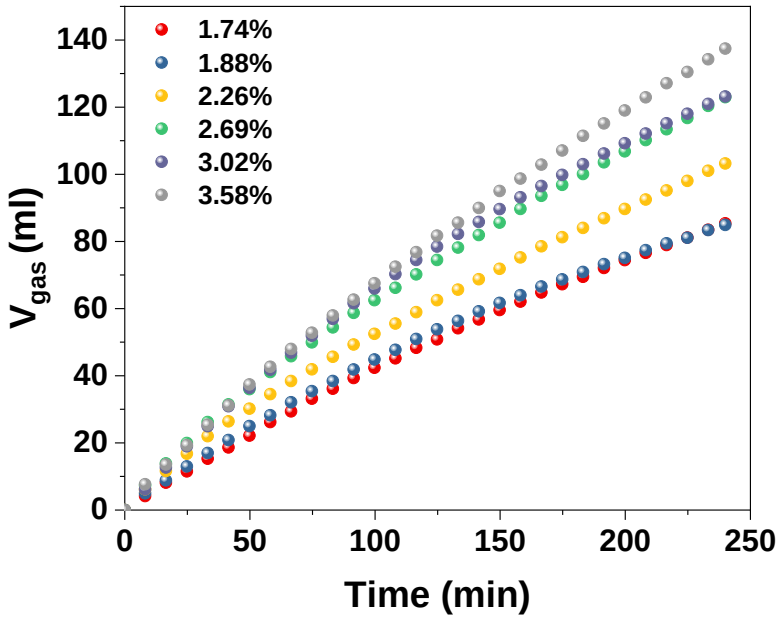

Figure S21. Plot of volume of produced gas versus time for the dehydrogenation of FA applying Co-SAs/NPs@NC-950 with different cobalt content.

In Line 256, we added the following text " The activities of the samples with different amounts of Co precursors were compared, too, and the highest activity is exhibited at an addition of 3.5 mol Co salt (Table S6 and Fig. S21)."

Question 3: Page 8 ln 118- Compare and discuss the surface area and pore size data with other 'related materials' as there are many examples e.g. ChemistrySelect 2022, 7, e202203273. ChemCatChem 2022, 14, e202101472. Scientific Reports 2017, 7, 39789.

Answer: Based on your suggestion, we have compared the surface area and pore size with other materials in the literature, see the following table. During pyrolysis, Zn nodes are reduced and volatilized (Zn, boiling point = 907 °C), which promotes the formation of porous structures.[21, 22] Co-SAs/NPs@NC-950 exhibited a higher specific surface area (1261 m^2/g) compared to other ZIF-derived NC materials, promoting the exposure of active sites.

Table S1. Comparison of surface area and pore size of different ZIF pyrolysis materials.

Catalysts	surface area ($m^2 \cdot g^{-1}$)	pore volume ($cm^3 \cdot g^{-1}$)	Reference
N-doped carbons (C-1000)	903	0.41	34
Fe-N-aRS$_{H3PO4}$	977	0.88	35
ZC50	1221.5	0.58	36
OP-Fe-NC	586.5	0.11	37
Co$_{NC-SA}$/N*-C	298.6	0.40	38
h-CoNC	293.5	0.11	39
Co-SAs/NPs@NC-750	787	0.32	
Co-SAs/NPs@NC-850	1068	0.36	This work
Co-SAs/NPs@NC-950	**1261**	**0.37**	

In Line 130, we modified the text to "Additionally, Co-SAs/NPs@NC-950 exhibits considerably higher Brunner-Emmett-Taylor (BET) surface area and pore volume (1261 m2·g-1 and 0.37 cm3·g-1) than the other samples and most of ZIF-derived NC materials (Fig. S7 and Table S1)."

Question 4: If the Co-SAs/NPs@NC-750 or 850 catalysts are heated at 950 °C for the appropriate time is the resulting material as active as Co-SAs/NPs@NC-950 and does it have the same textural properties.

Answer: Materials obtained by further heating Co-SAs/NPs@NC-750 or -850 at 950°C for 1h did not achieve the same activity and textural properties as Co-SAs/NPs@NC-950. After heating at 950°C for 1 h, the activity of Co-SAs/NPs@NC-750 or -850 catalysts was slightly worse than that of Co-SAs/NPs@NC-950, but better than that original samples as shown in Figure S17.

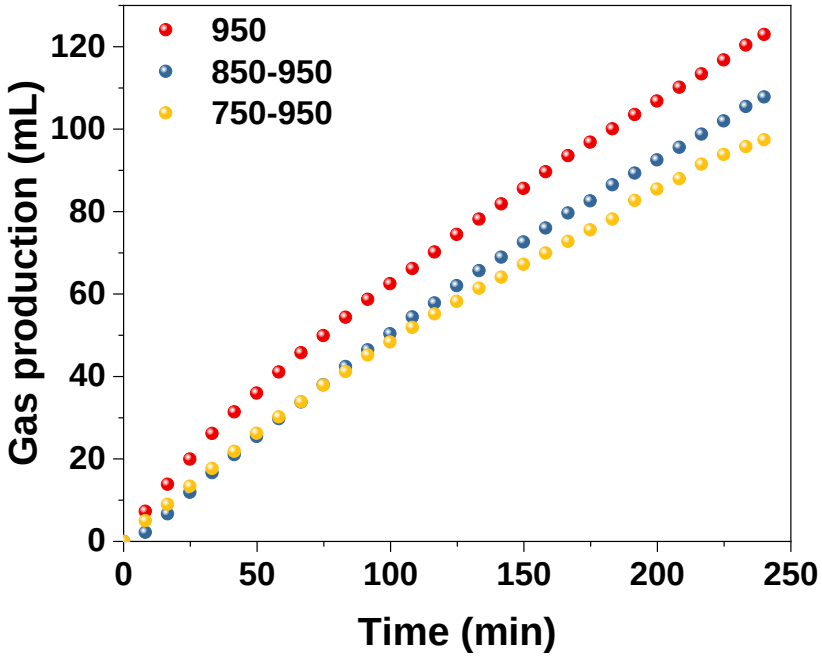

Figure S17. Plot of volume of produced gas versus time for the dehydrogenation of FA applying Co-SAs/NPs@NC-950, Co-SAs/NPs@NC-850 and Co-SAs/NPs@NC-750 after heating at 950 °C.

In order to better analyze the activity differences, BET, XRD and Raman were done to explore the textural features of Co-SAs/NPs@NC-750 or -850 after heating at 950°C and correlate them with the activity. The BET specific surface area of Co-SAs/NPs@NC-950 (1261 $m^2 \cdot g^{-1}$) was significantly higher than Co-SAs/NPs@NC-750 or -850 after heating at 950°C. The specific surface area of the sample after heating at 950°C was slightly higher than that of before reheating, which would promote the exposure of active sites.

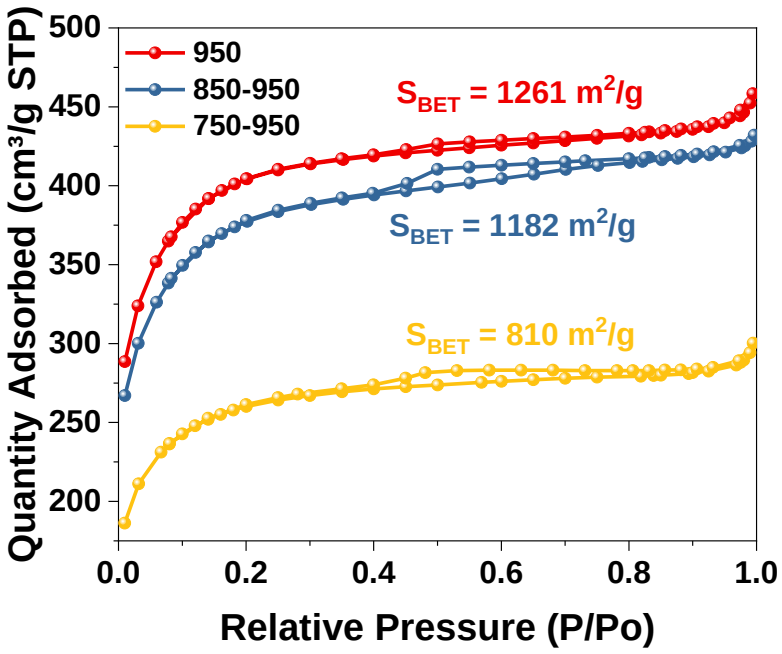

Figure S18. N_2 Adsorption isotherm of Co-SAs/NPs@NC-950, Co-SAs/NPs@NC-850 and Co-SAs/NPs@NC-750 after heating at 950 °C.

XRD plots of Co-SAs/NPs@NC-750 or -850 after heating at 950°C show characteristic peaks of metallic Co due to the aggregation of some cobalt species, proving that the activity enhancement after reheating was related to the appearance of nanoparticles. However, the appearance of characteristic peaks of graphitic carbon was not observed at 26.2° (Figure S19) and the D and G peaks in the Raman spectrum were broader, indicating the absence of graphitic carbon (Figure S20). These prove that the excellent activity of Co-SAs/NPs@NC-950 is associated with graphitic carbon due to the promotion of electron transfer between nanoparticles and single atoms as evidenced by DFT calculations.

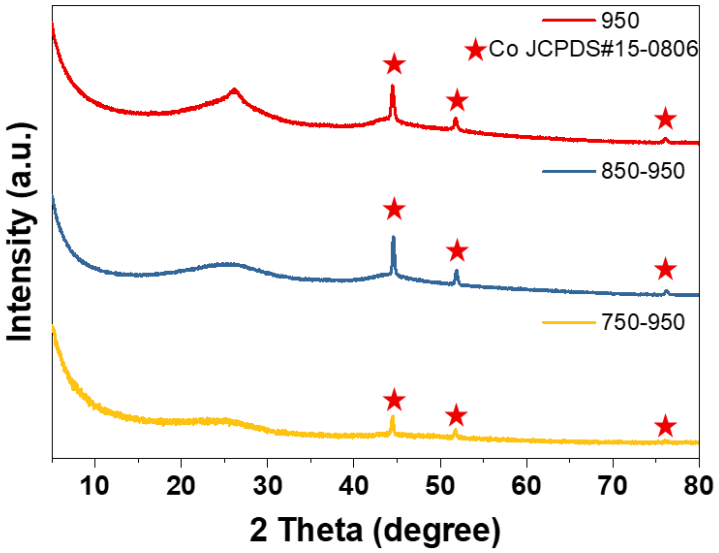

Figure S19. XRD spectra of Co-SAs/NPs@NC-950, Co-SAs/NPs@NC-850 and Co-SAs/NPs@NC-750 after heating at 950 °C.

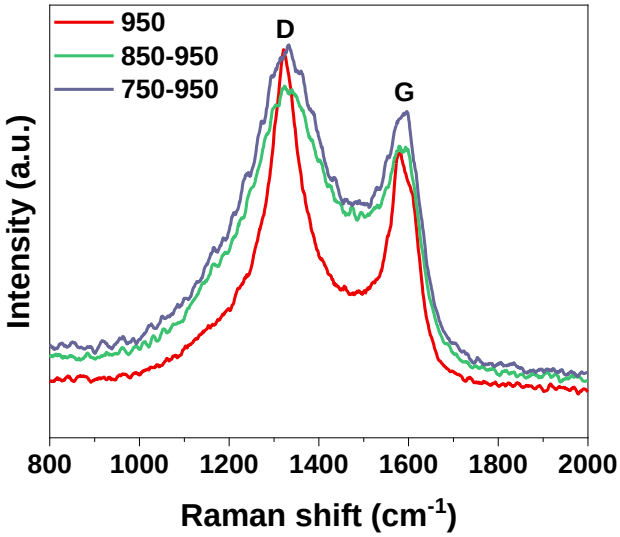

Figure S20. Raman spectra of Co-SAs/NPs@NC-950, Co-SAs/NPs@NC-850 and Co-SAs/NPs@NC-750 after heating at 950 °C.

Overall, the samples showed recovered activity after reheating 950 °C, which correlates with the appearance of nanoparticles and the increase in specific surface area. However, the activity still did not reach the same level as Co-SAs/NPs@NC-950, which is related to the lower specific surface and absence of graphitic carbon that facilitates electron transfer between nanoparticles and single atoms. The above results further

demonstrate the synergistic effect of N-doped graphite-like carbon-encapsulated nanoparticles and single atoms.

In Line 250, we added the text "In addition, Co-SAs/NPs@NC-850 and Co-SAs/NPs@NC-750 were pyrolyzed a second time at 950°C for 1 h, which showed an increase in activity but lower than Co-SAs/NPs@NC-950 (Fig. S17). Structural characterization of these materials shows the presence of Co nanoparticles in the re-pyrolyzed samples, but the low specific surface and the absence of graphite-like carbon resulted in lower activity compared to Co-SAs/NPs@NC-950 (Fig. S18-S20)."

Question 5: Page 10 ln 197- least squares

Answer: In Line 224, we corrected the text to "least squares".

Question 6: Pg 11 ln 204- can the evolution of the catalyst be monitored using VT XRD.

Answer: Based on your suggestions, we have supplemented the VTXRD of Co doped-ZIF (pyrolysis from room temperature to 950 ℃) to monitor the catalyst evolution. The XRD patterns of CoZn-ZIF are in agreement with the literature, and it is thermally stable up to 550 °C.[40, 41] After the pyrolysis temperature reached 650 ° C, the XRD patterns changed significantly due to the collapse of the ordered crystal structure of ZIFs.[42] As the temperature increases further, X-ray diffraction (XRD) patterns of Co-SAs/NPs@NC-850 and Co-SAs/NPs@NC-750 revealed two broad peaks at 20-30° and 40-50°, representing the amorphous carbon peaks.[7] Notably, three characteristic peaks with 2θ values located at 44.2°, 51.5°, and 75.8° were observed only in the XRD patterns of Co-SAs/NPs@NC-950, attributed to diffraction from the (111), (200), and (220) crystal planes of metallic cobalt (JCPDS #15-0806), suggesting the formation of Co nanoparticles.[8, 9] In the XRD spectra of Co-SAs/NPs@NC-950, the peak with a 2θ value of 26.2° (JCPDS #41-1487) belongs to graphitic carbon.[10-12]

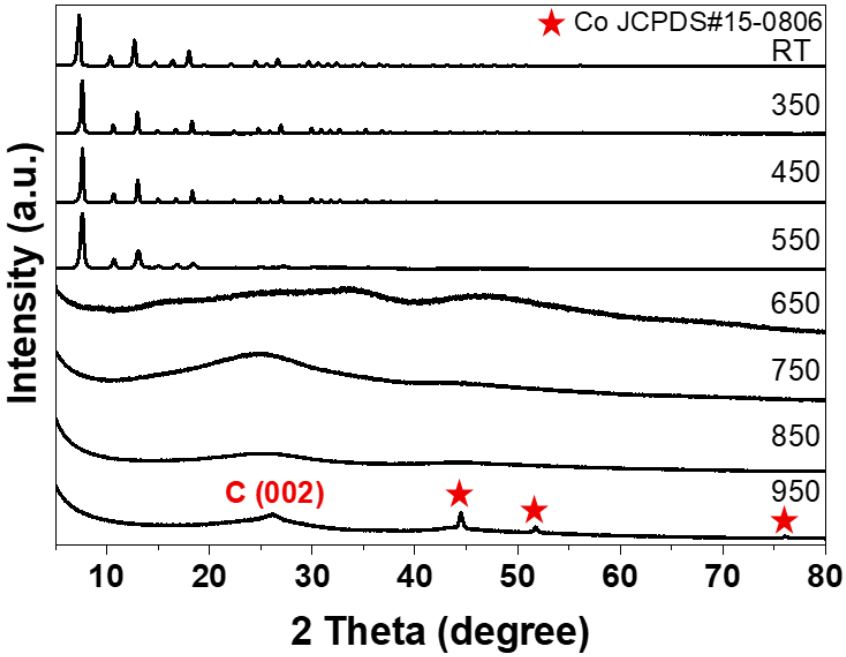

Figure S4. VTXRD spectra of cobalt-doped ZIF with pyrolysis temperatures ranging from room temperature to 950 °C.

In Line 115, we added the following text " Variable temperature powder X-ray diffraction (VTXRD) was performed to monitor the catalyst evolution. After the pyrolysis temperature reached 650 °C, the XRD patterns changed significantly due to the collapse of the ordered crystal structure of ZIFs (Fig. S4).39 As the temperature increases further, XRD patterns of Co-SAs/NPs@NC-850 and Co-SAs/NPs@NC-750 revealed two broad peaks at 20-30° and 40-50°, representing the amorphous carbon peaks (Fig. S5).40 Notably, three characteristic peaks at 44.2°, 51.5°, and 75.8°, belonging to metallic cobalt (JCPDS #15-0806) and the peak at 26.2° belonging to graphitic carbon (JCPDS #41-1487) were observed only in the XRD spectra of the Co-SAs/NPs@NC-950, suggesting that graphite-like encapsulated cobalt nanoparticles appeared on the catalyst."

Question 7: Pg 12 ln 222-225- More detail required here on the additional catalysts. How did the composition and textural properties of the catalyst change as a function of the pyrolysis time i.e. can any conclusions be made about why 0.5 h, 1 h and 2 h differ?

For instance, N_2 adsorption data, XPS and HAADF-STEM should be provided for the catalyst generated after 30 min to explore the difference in performance.

Answer: Based on your suggestions, we have added the following characterizations (HAADF-STEM, XRD, BET, XPS) for Co-SAs/NPs@NC-950-1h, Co-SAs/NPs@NC-950-0.5h and Co-SAs/NPs@NC-950-2h to clarify the effect of pyrolysis time on catalyst structure and activity. As can be seen from the XRD patterns, Co-SAs/NPs@NC-950-0.5h shows characteristic peaks of amorphous carbon, and as the pyrolysis time is increased, Co-SAs/NPs@NC-950-1h and Co-SAs/NPs@NC-950-2h show characteristic peaks of Co metal (JCPDS #15-0806) and small sharp peaks with a 2θ value of 26.2° belongs to graphitic carbon (JCPDS #41-1487). During high temperature pyrolysis, individual cobalt metal sites aggregate to form Co metal particles, which are widely believed to promote the degree of graphitization of carbon matrix. [43, 44]

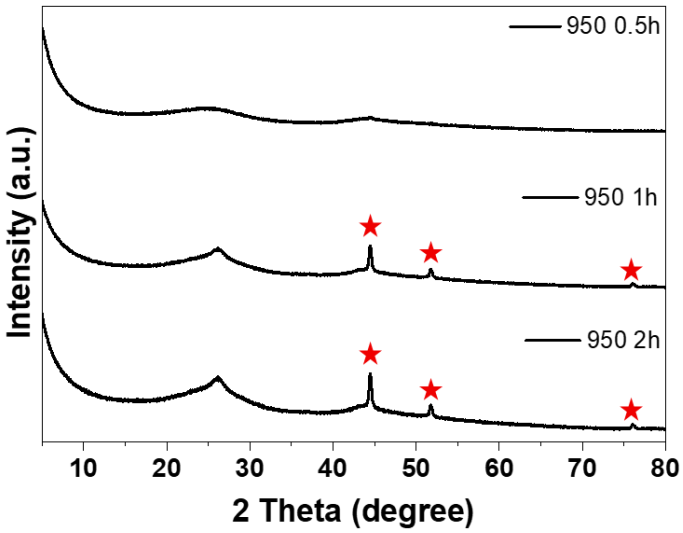

Figure S24. XRD spectra of Co-SAs/NPs@NC-950-1h, Co-SAs/NPs@NC-950-0.5h and Co-SAs/NPs@NC-950-2h.

As the pyrolysis time increases, the specific surface area of the sample gradually increases. Co-SAs/NPs@NC-950-2h exhibited the largest specific surface area (1364 m^2/g), compared to SAs/NPs@NC-950-1h (1261 m^2/g) and SAs/NPs@NC-950-0.5h (1013 m^2/g).

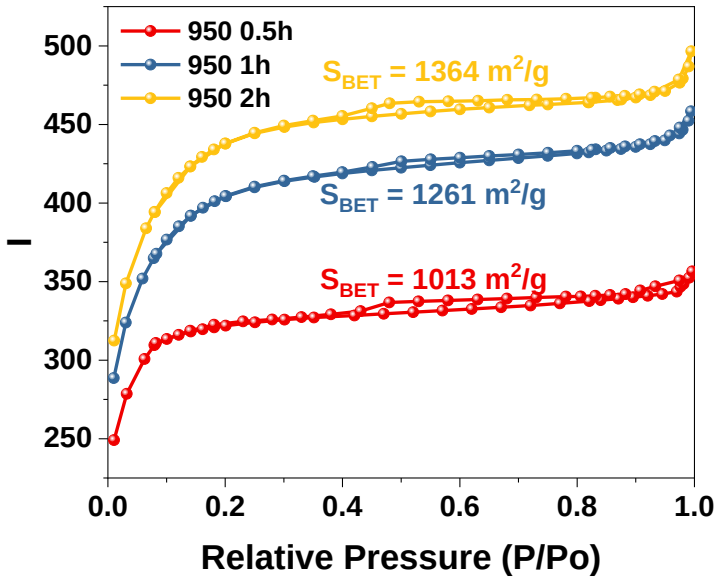

Figure S25. N_2 Adsorption isotherm of Co-SAs/NPs@NC-950-1h, Co-SAs/NPs@NC-950-0.5h and Co-SAs/NPs@NC-950-2h.

As the pyrolysis time increases, the particle size of cobalt species gradually increases, too. Only atomically dispersed cobalt was observed in the Co-SAs/NPs@NC-950-0.5h. For the 1h sample, 7.5 ± 1.7 nm of cobalt nanoparticles and atomically dispersed cobalt appeared, while for the 2h sample, the size of the nanoparticles changed to 12.7 nm. Therefore, the introduction of nanoparticles will strengthen the original single atomic sites, but the size of the nanoparticles should not be too large, otherwise it will lead to poor activity.

The graphite-carbon structure is not easy to see in HAADF for the following reasons: the C atomic number is low, and the imaging quality is a little worse, but the HRTEM is much better. In addition, for amorphous structures, HAADF does not proof a lattice image.

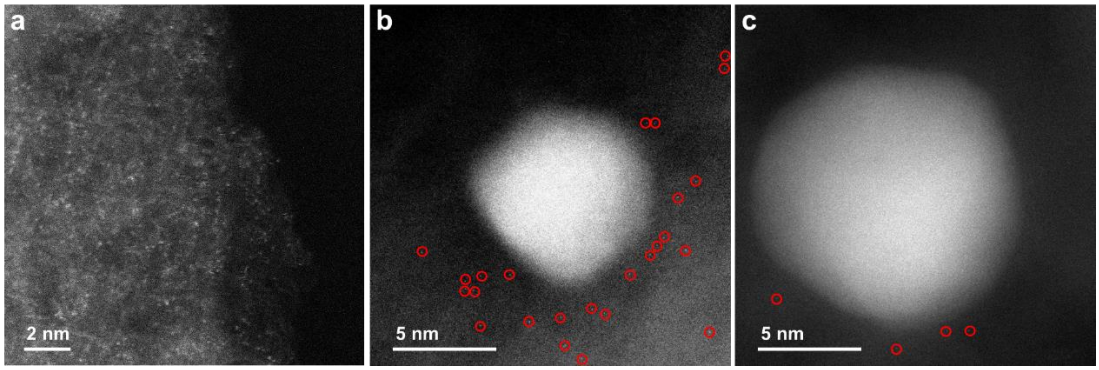

Figure S26. HAADF-STEM image of Co-SAs/NPs@NC-950-0.5h, Co-SAs/NPs@NC-950-1h and Co-SAs/NPs@NC-950-2h. Cobalt single atoms are marked with red circles.

XPS spectra show that the Co-N content of the samples decreases with increasing pyrolysis time (for 0.5h, 1h, and 2h the values are 24.4%, 17.6%, and 15.3%, respectively). The poor activity of Co-SAs/NPs@NC-950-0.5h is attributed to the absence of nanoparticle modulation of atomic sites, and the poor activity of Co-SAs/NPs@NC-950-2h is attributed to the sintering of Co atoms with increasing pyrolysis time, leading to a loss of active Co-N sites.

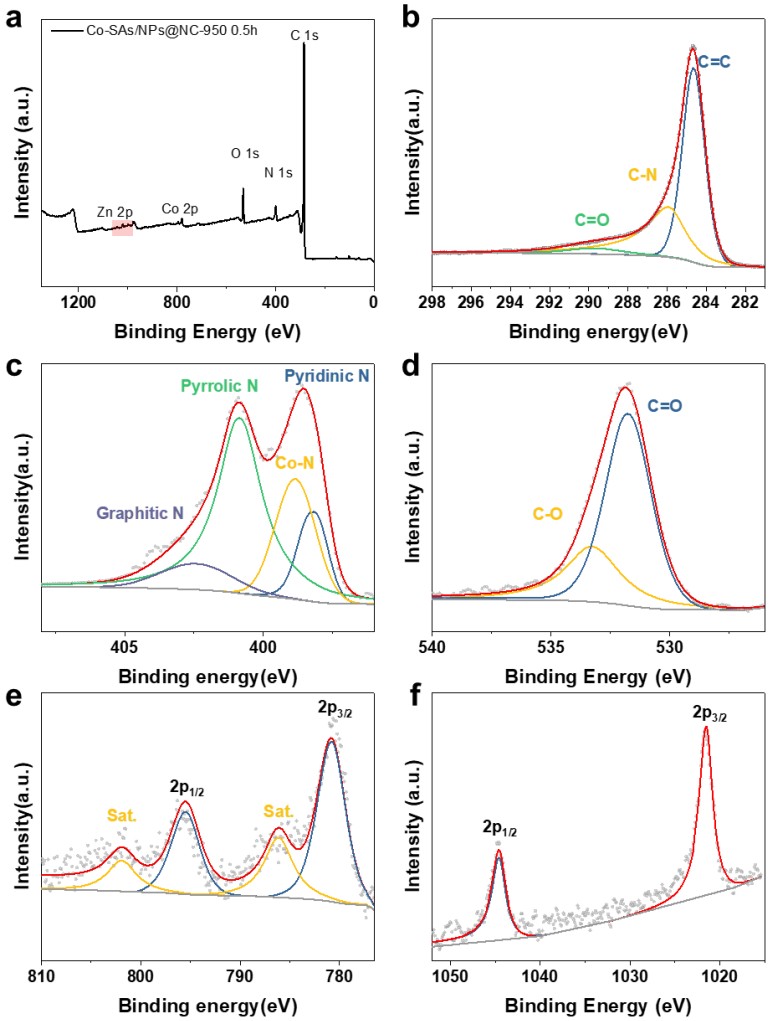

Figure S27. a XPS survey scanning. **b** C 1s. **c** N 1s. **d** O 1s. **e** Co 2p. and **f** Zn 2p spectra of Co-SAs/NPs@NC-950-0.5h.

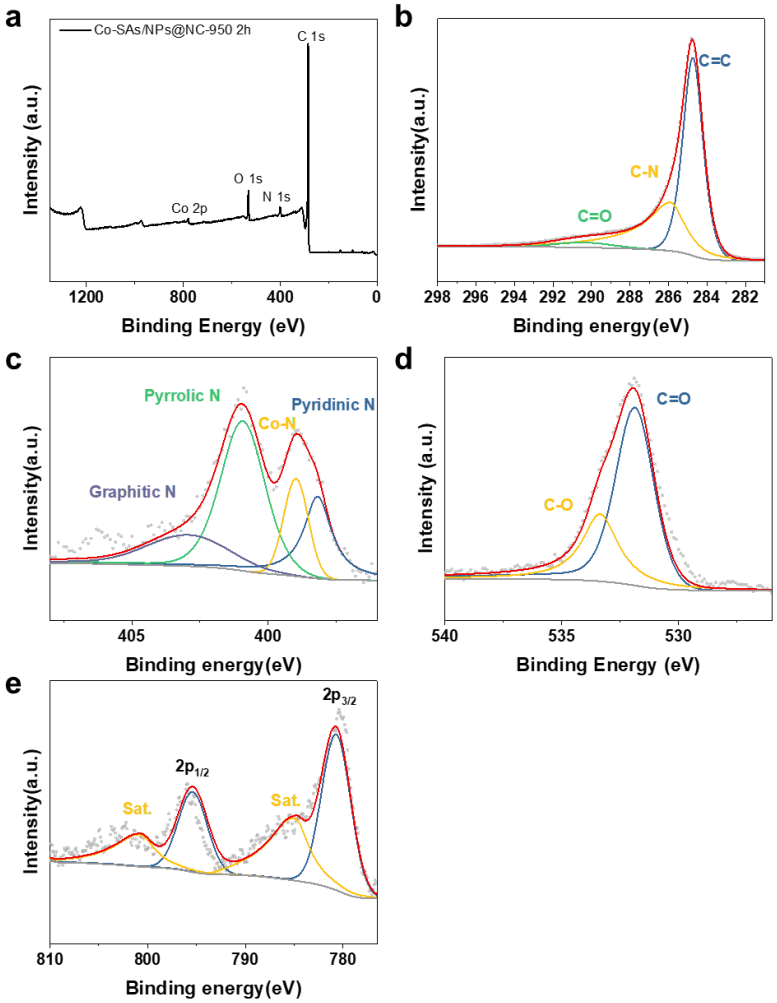

Figure S28. a XPS survey scanning. **b** C 1s. **c** N 1s. **d** O 1s. and **e** Co 2p spectra of Co-SAs/NPs@NC-950-2h.

Table S7. The atomic percentages of each substance of Co-SAs/NPs@NC-950-1h, Co-SAs/NPs@NC-950-0.5h and Co-SAs/NPs@NC-950-2h.

Catalysts	C/%	N/%	O/%	Co/%	Zn/%
Co-SAs/NPs@NC-950-1h	87.73	4.02	7.80	0.46	0
Co-SAs/NPs@NC-950-0.5h	86.35	5.92	6.90	0.63	0.21
Co-SAs/NPs@NC-950-2h	88.71	4.54	6.21	0.54	0

In summary, with increasing pyrolysis time, the XRD characteristic peaks of cobalt and graphitic carbon appear, the specific surface area increases, the particle size of

cobalt species increases, and the number of single-atom Co-N site gradually decreases. ***In Line 263, we added the following text "The structural characterization of the materials showed that with the prolongation of pyrolysis time, the content of Co-N single atom sites gradually decreased due to the aggregation of metal atoms into nanoparticles, which explains the difference in activity between the samples with pyrolysis time of 0.5 h, 1 h and 2 h (Fig. S24-S28 and Table S7). "***

Question 8: Figure S12 – is this the plot for catalyst generated at Co-SAs/NPs@NC-950? if so, include catalyst details in the caption.

Answer: Figure S12 shows the Plots of the volume of gas generated utilizing Co-SAs/NPs@NC-950. Because of added data in the revised manuscript this Figure is now Figure S23.

We modified the subheading of Figure S23 to "Plots of the volume of gas formed from FA versus time using Co-SAs/NPs@NC-950 prepared with different pyrolysis times at 950 °C. "

Question 9: Page 12 ln 234- Fig S13 shows a marked enhance in TOF in the early stages of the reaction with sodium formate as additive (up to ca. 20 min). The authors should comment as it would be an ideal system if the subsequent drop in TOF could be overcome. The caption in Fig S13 should also include the catalyst.

Answer: Thanks for the advice and we agree with your point of view. It is well known that HCOOH dehydrogenation following the formate pathway mainly includes three elementary reaction steps: (I) HCOOH is adsorbed on the active site, (II) the removal of H by two dehydrogenation pathways, the formate pathway (S3, S4) and (III) the combination of two adsorbed H* to form H_2.

$$HCOOH^* + * \rightarrow HCOO^* + H^* \quad (S3)$$

$$HCOO^* \rightarrow CO_2{}^* + H^* \quad (S4)$$

H_2 evolution upon FA dehydrogenation could be significantly improved by the addition of HCOONa to the reaction system, because the excess adsorbed $HCOO^-$ acts

as a reaction intermediate for FA dehydrogenation.[45, 46] Indeed, when sodium formate was used as an additive, Co-SAs/NPs@NC-950 showed better gas precipitation rates in the first 30 minutes, but the activity decreased with time.[47] At the same time, it was observed that the solution color changed from colorless to pink, which was related to the partial loss of Co. Therefore, we chose PC without additives as catalyst stable reaction conditions. If the subsequent drop in TOF can be overcome, this would be an ideal system and will be investigated further in subsequent studies.

In Fig S29, we modified the subheading to "Reaction conditions: FA (10 mmol, 377 μL), additive (1.0 mmol), Co-SAs/NPs@NC-950 (30 mg) in specified solvents (6 mL), T_{set}: 110 °C, T_{actual}: 98 °C, 4 h."

Question 10: Page 12 ln 236- The authors should explain the kinetics of hydrogen release as a function of the catalyst concentration in terms of reaction order and its interpretation. Again, add the catalyst to the caption rather than assume the reader knows.

Answer: As suggested we complemented the kinetics of the formic acid dehydrogenation reaction at different cobalt contents and investigated the correlation between the reaction rate and cobalt content. We also added the catalyst structure to the caption. Since ln(dV/dt) is linearly correlated with t, the kinetic study of hydrogen release is a first-order reaction kinetics for formic acid dehydrogenation.[48] However, the slopes of several curves were not the same at different cobalt concentrations, suggesting that the kinetics depend not only on formic acid but also on the active metal centers.

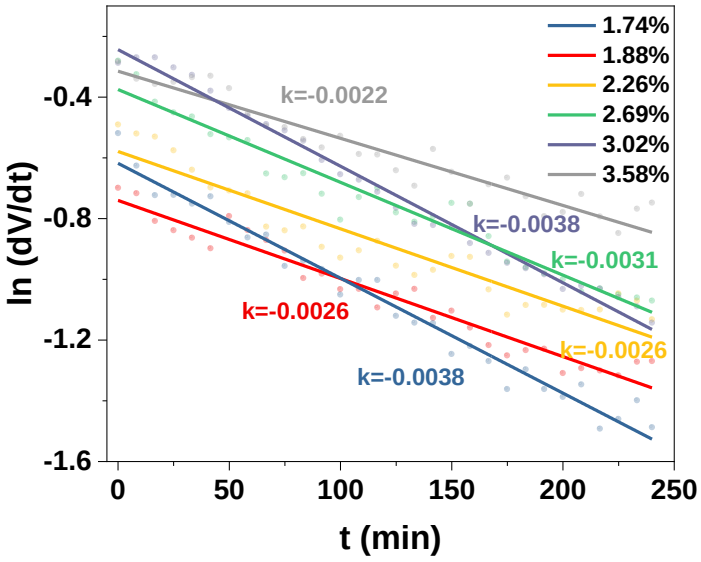

Figure S37. Kinetics of hydrogen release reaction at different cobalt contents.

In the next study of the reaction rate versus cobalt content, the kinetic reaction order to cobalt content at low levels (less than 2.5%) appeared at 1.02[49], suggesting that the almost uniformly distributed Co single atom sites are the major active sites. When the Co species content reaches 2.7%, a sudden increase in r occurs, indicating that the nanoparticles synergize well with the single atoms. As the Co species content continues to increase, the curve becomes non-linear, related to the increase of nanoparticles and the decrease of single atomic sites.

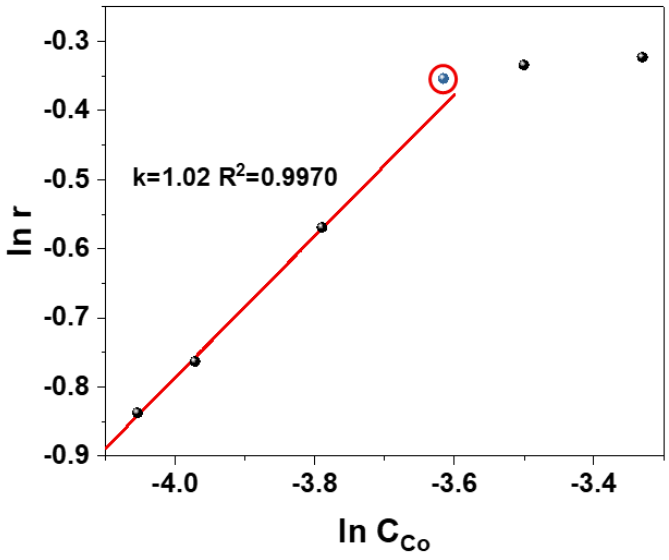

Figure S38. Kinetic reaction order to cobalt concentration during formic acid dehydrogenation over Co-SAs/NPs@NC-950 catalyst.

XRD patterns of the samples with different cobalt contents showed that the three samples above 2.5% exhibited characteristic peaks of cobalt metal, while the three samples with cobalt contents below 2.5% did not. At very low levels of cobalt, no nanoparticles were observed, and as the cobalt content increased, nanoparticles gradually appeared, which is consistent with the above conclusions.

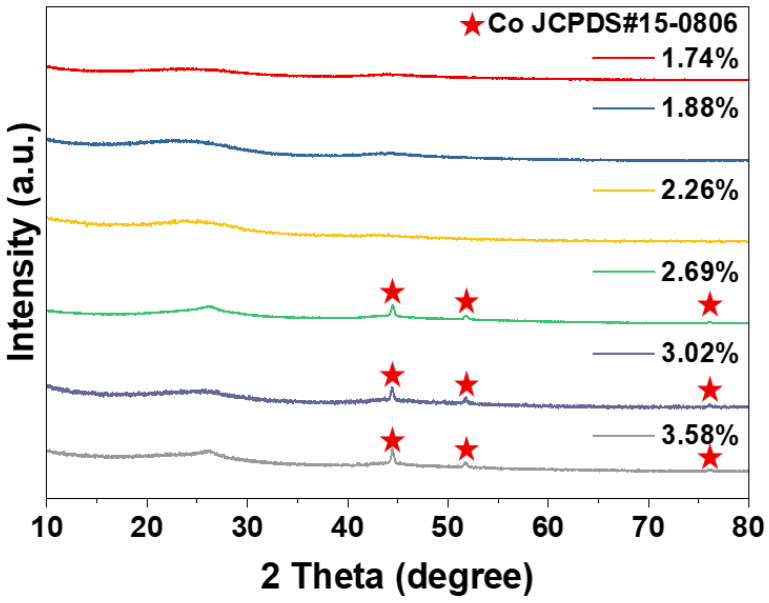

Figure S39. XRD spectra of Co-SAs/NPs@NC-950 catalyst with different cobalt contents.

In ***Line 312***, ***We added the following text "The kinetics of the reaction demonstrated that hydrogen release followed first-order reaction kinetics, but the slopes of several curves were not the same at different cobalt content, suggesting that the kinetics depended not only on formic acid but also on the active center (Fig. S37). Further kinetic studies showed that the kinetic reaction order to cobalt content appeared at 1.01 at low levels (less than 2.5%), considering the absence of cobalt metal peaks in XRD, which suggests that the almost uniformly distributed cobalt single-atom sites are the main active sites (Fig. S38 and S39). When the Co species content reaches 2.7%, a sudden increase in the reaction rate r occurs, indicating a synergistic effect of the present nanoparticles on the catalyst activity. As the Co species content continues to increase, the curve becomes nonlinear, due to the increase of nanoparticles and the decrease of isolated metal sites."***

Question 11: Page 13 ln 241- compare the apparent activation energy to related system in the literature and discuss.

Answer: Based on your suggestion, we have compared the apparent activation energy to related system in the literature, see the following table. Co-SAs/NPs@NC-950 also exhibited activation energy values comparable to those of noble metal catalysts (Pd-WOx/NPCC). However, there is still a gap with precious metals due to the limitations of PC solvents and low-cost metal cobalt.

Table S10. Comparison of the apparent activation energy of different materials.

Catalysts	apparent activation energy (KJ/mol)	Reference
Pd–WOx/NPCC	87.9	50
$Pd_{0.6}Au_{0.4}$@CTF	41.2	51
Pd/C	42	52
Pd@Bi/C	44	52
$Pd_{60}Au_{40}$/HPC-NH_2	64.8	53

PdAg-MnO_x/N-SiO_2	72.4	54
Co-SAs/NPs@NC-950	**88.4**	**This work**

In ***Line 284***, ***We added to "The activation energy was calculated to be 88.4 kJ/mol, which is even comparable to noble metal catalysts (Fig. S31 and Table S10)."***

Question 12: Page 15 ln 292- Can the authors describe more clearly what they mean by the carbonate pathway (maybe include a figure) as I understand the formate HC(O)O and thought the other C(O)OH was carboxyl. Please clarify.

Answer: Sorry, we made a mistake here, it should be carboxylate pathway, not carbonate pathway. Formic acid dehydrogenation can proceed through two main pathways, namely formate (HCOO) and carboxyl (COOH), with the latter potentially leading to the formation of CO on the surface.[55]

In Line 349 and 352, we corrected the text to "carboxylate pathway".

Question 13: Page 16 ln 319- Can the authors comment on whether the hydrogen released from DC(O)OH is all HD or a mixture of isotopomers.

Answer: We complemented the dehydrogenation experiments with DCOOH, and mass spectrometry analysis showed that HD was detected as the dominating product, as well as a small amount of H_2. Accordingly, surface hydride and hydrogen atoms from HCOO* are combined to form H_2.[56]

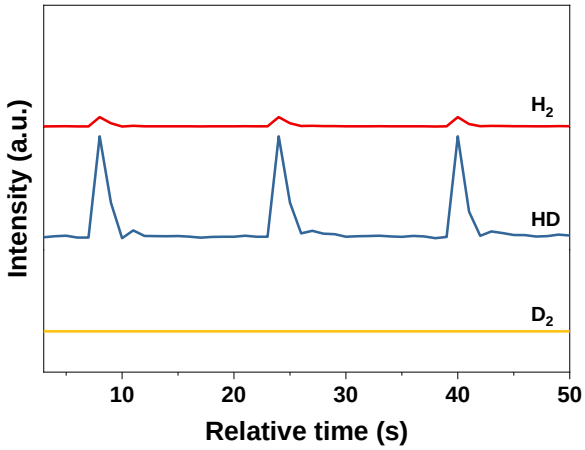

Figure. Detection of H_2, HD and D_2 by mass spectroscopy. Reaction conditions: DCOOH (10 mmol, 377 μL), Co-SAs/NPs@NC-950 (30 mg), PC (6 mL), Tset: 110 °C, Tactual: 98 °C.

Question 14: Pages 18-19- The authors correlate the elevated d band center (to -0.67 eV) with and enhanced adsorption and activation of intermediates but it's not clear why or how this occurs as C-H cleavage of the formate is the RDS, so how is this facilitated? It's not clear in the TS from the DFT calculations how activation of this C-H occurs and why it is facilitated for the NP system. Is it associated with the depletion of electrons on the Co site?

Answer: In response to each of your four questions, we answer them as follows.

Association of the elevated d-band center with enhanced intermediate adsorption and activation:

The elevated d-band center implies an elevated energy of the metal d-orbitals, which leads to enhanced interactions between the metal and the adsorbed molecules. In our study, the upshift of the d-band center could be caused by the size effect of nanoparticles or surface modification. This upshift makes the electronic structure of the metal surface more favorable to overlap with the orbitals of the intermediates, which enhances the adsorption and subsequent activation process.

Activation mechanism of C-H bond breaking:

In the DFT calculations, we observe that the C-H bond of the formate molecule is elongated in the transition state (from 1.10 Å to 1.15 Å) due to the formation of chemical bonds between the d electrons on the metal surface and the carbon and

hydrogen atoms in the formate, which indicates that it is being activated.

Facilitation of C-H bond activation by nanoparticles:

Nanoparticles can provide more active sites for adsorption and activation of reactants due to their small size effect and high specific surface area. In addition, the edge and corner sites of nanoparticles usually have higher catalytic activity, which also helps to reduce the activation energy for C-H bond breaking.

Electron reduction in relation to C-H bond activation:

During the reaction, electrons on the metal sites may be partially transferred to the adsorbed molecules, which may indeed affect the activation of the C-H bond. However, in our study, electron reduction is not the main reason for directly promoting C-H bond breaking. Instead, we believe that it is the interaction between the metal and the adsorbed molecule as well as the size effect of the nanoparticles that together lead to the activation of the C-H bond.

In summary, the upward shift of the d-band center, the size effect of the nanoparticles, and the interaction between the metal and the adsorbed molecules jointly promote the C-H bond breaking in formate. We appreciate your feedback and will further study the specific mechanism in subsequent studies.

Question 15: Page 19- relates to the point above (which I accept may reflect my lack of understanding). Could the enhancement in activity for the Co-SAs/NP-950 system be associated with the different coordination environments at the single atom i.e. the C_2N_2Co rather than the CoN_4 associated with the less active catalysts (and thereby not due to the NP other than it is required to change the C/N ratio and thereby the coordination at Co). This does not appear to have been explored by calculations as the Co SAs model was CoN_2C_2 rather than CoN_4. Is it worth performing these calculations to compare?

Answer: CoN_4 modeling is not required for the following reasons. In previous studies, we conducted a coordination effect study and found that Co-N-C with CoN_2 by gradient pyrolysis up to 1000 °C in an argon atmosphere showed better activity compared to CoN_3 and CoN_4.[3] On the basis of this, in the present study we found that the coexistence

of nanoparticles and single atom promotes better formic acid dehydrogenation due to the reinforcement of single atoms by nanoparticles. XAFS showed that the coordination environment of the single-atom cobalt site happens to be Co_2N_2, so we chose this model to calculate. Interestingly, the single atom units in Co-SAs/NPs@NC-850 and Co-SAs/NPs@NC-750 in our study are CoN_3 and CoN_4, respectively. In combination with our study, the following ordering of activities can be derived: Co-SAs/NPs@NC>CoN_2C_2>CoN_4. Therefore, we introduced nanoparticles on the best available CoN_2C_2 catalyst to study their effect and achieve enhanced formic acid dehydrogenation. Only the best Co SAs model was CoN_2C_2 and Co-SAs/NPs@NC model should be calculated to clarify the role of nanoparticles.

Response to Reviewer 3:

Reviewer 3's comments: Shi et al have reported the dehydrogenation of formic acid utilizing cobalt based single atom catalysts with their activity synergistically increased by combining them with nanoparticles. The catalytic system can be typically considered as a hybrid system consisting of nanoparticles and single-metal sites. Three different set of Co-SAs/NPs@NC were synthesized based on the pyrolysis temperature (750°C, 850°C and 950°C) and the desired catalytic system having both nanoparticles and single atom catalytic sites were found only in Co-SAs/NPs@NC-950. All the three systems were studied for their catalytic activity and all systems showed better behaviour compared to standard commercial noble metal catalysts (Pd/C and Pt/C) with Co-SAs/NPs@NC-950 providing the best results. The catalyst was found to be stable in long term tests with no significant cobalt leaching. Furthermore, the dehydrogenation v/s dehydration reaction showed selectivity up to 99.96%. The formic acid dehydrogenation mechanism is believed to exclusively follow the formate ion mechanism instead of carbonate ion mechanism based on DRIFT, KIE and DFT studies. The report provides deep insight into the synergistic effect of nanoparticles on the catalytic activity of cobalt based single atom catalysts for dehydrogenation of formic acid. The results are well supported by experimental and theoretical data and can open new opportunities in understanding how the catalytic performance can be enhanced by synergistic action of metal sites of different sizes.

Based on above mentioned reasons, this manuscript can be published in Nature Communications

Our response: We thank the referee for the positive comments.

Question 1: While discussing solvent screening, abbreviation for propylene carbonate (PC) has been directly used and it is not clear which solvent has been used. The authors should mention the name of the solvent instead of directly using the abbreviation form.

Answer: Thank you for the suggestion. We have now introduced this solvent with the full name in the abstract.

Question 2: while discussing cobalt content in 3 different types of catalysts; Co-SAs/NPs@NC-750 should be written after Co-SAs/NPs@NC-850 (in decreasing order of the pyrolysis temperature) as the same trend is followed throughout the whole manuscript.

Answer: We have changed all the sections in the manuscript comparing the three different types of catalysts with the order of decreasing pyrolysis temperature, i.e., Co-SAs/NPs@NC-950, Co-SAs/NPs@NC-850 and Co-SAs/NPs@NC-750

In Line 133, we modified the text to "Atomic absorption spectroscopy (AAS) shows cobalt contents of 2.69 wt%, 2.74 wt% and 2.73 wt% in Co-SAs/NPs@NC-950, Co-SAs/NPs@NC-850, and Co-SAs/NPs@NC-750, respectively.".

In Line 244, we modified the text to "As shown in Fig. 3a, Co-SAs/NPs@NC-950 exhibited significantly higher activity than Co-SAs/NPs@NC-850 and Co-SAs/NPs@NC-750."

References

1. Liu M*, et al.* Heterogeneous catalysis for carbon dioxide mediated hydrogen storage technology based on formic acid. *Adv. Energy. Mater.* **12**, 2200817 (2022).
2. Sordakis K*, et al.* Homogeneous catalysis for sustainable hydrogen storage in formic acid and alcohols. *Chem. Rev.* **118**, 372-433 (2018).
3. Li X*, et al.* Cobalt single-atom catalysts with high stability for selective dehydrogenation of formic acid. *Angew. Chem. Int. Ed.* **59**, 15849-15854 (2020).
4. Wang W, Chen D, Li F, Xiao X, Xu Q. Metal-organic-framework-based materials as platforms for energy applications. *Chem* **10**, 86-133 (2024).
5. Huang H*, et al.* Rapid and energy-efficient microwave pyrolysis for high-yield production of highly-active bifunctional electrocatalysts for water splitting. *Energy Environ. Sci.* **13**, 545-553 (2020).
6. Liu P*, et al.* Synergy between palladium single atoms and nanoparticles via hydrogen spillover for enhancing CO_2 photoreduction to CH_4. *Adv. Mater.* **34**, 2200057 (2022).
7. An Z*, et al.* Highly active, ultra-low loading single-atom iron catalysts for catalytic transfer hydrogenation. *Nat. Commun.* **14**, 6666 (2023).
8. Zhang T*, et al.* Co@C nanorods as both magnetic stirring nanobars and magnetic recyclable nanocatalysts for microcatalytic reactions. *Appl. Catal. B* **304**, 120925 (2022).
9. Tian H*, et al.* High-power lithium-selenium batteries enabled by atomic cobalt electrocatalyst in hollow carbon cathode. *Nat. Commun.* **11**, 5025 (2020).
10. Zhu Z*,* et al. Carbon-supported Co/Co_3O_4 hybrid catalyst: an efficient non-noble metal catalyst for the hydrodeoxygenation of vanillin. *Catal. Sci. Technol.* **13**, 6233-6237 (2023).
11. Jin H*, et al.* In situ cobalt-cobalt oxide/N-doped carbon hybrids as superior bifunctional electrocatalysts for hydrogen and oxygen evolution. *J. Am. Chem.*

Soc. **137**, 2688-2694 (2015).

12. Jiang SF, *et al.* High efficient removal of bisphenol A in a peroxymonosulfate/iron functionalized biochar system: Mechanistic elucidation and quantification of the contributors. *Chem. Eng. J.* **359**, 572-583 (2019).
13. Wang A, Zhao C, Yu M, Wang W. Trifunctional Co nanoparticle confined in defect-rich nitrogen-doped graphene for rechargeable Zn-air battery with a long lifetime. *Appl. Catal. B* **281**, 119514 (2021).
14. Wei J, *et al.* Site-specific metal-support interaction to switch the activity of Ir single atoms for oxygen evolution reaction. *Nat. Commun.* **15**, 559 (2024).
15. Wu Z, *et al.* Facilely tuning the first-shell coordination microenvironment in iron single-atom for fenton-like chemistry toward highly efficient wastewater purification. *Environ. Sci. Technol.* **57**, 14046-14057 (2023).
16. Liu Y, Xue JS, Zheng T, Dahn JR. Mechanism of lithium insertion in hard carbons prepared by pyrolysis of epoxy resins. *Carbon* **34**, 193-200 (1996).
17. Alexander LE, Sommer EC. Systematic analysis of carbon black structures. *J. Phys. Chem. C* **60**, 1646-1649 (1956).
18. Santos JL, Megías-Sayago C, Ivanova S, Centeno MÁ, Odriozola JA. Structure-sensitivity of formic acid dehydrogenation reaction over additive-free Pd NPs supported on activated carbon. *Chem. Eng. J.* **420**, 127641 (2021).
19. Zhang S, Jiang B, Jiang K, Cai W B. Surfactant-free synthesis of carbon-supported palladium nanoparticles and size-dependent hydrogen production from formic acid-formate solution. *ACS Appl. Mater. Interfaces* **9**, 24678-24687 (2017).
20. Zhang C, *et al.* Unraveling the role of zinc on bimetallic Fe_5C_2-ZnO catalysts for highly selective carbon dioxide hydrogenation to high carbon α-Olefins. *ACS Catal.* **11**, 2121-2133 (2021).
21. Wang Z, *et al.* Atomically dispersed Co_2-N_6 and Fe-N_4 costructures boost oxygen reduction reaction in both alkaline and acidic media. *Adv. Mater.* **33**, 2104718 (2021).

22. Xue Y*, et al.* MOF-derived Co and Fe species loaded on N-doped carbon networks as efficient oxygen electrocatalysts for Zn-Air batteries. *Nano Micro Lett.* **14**, 162 (2022).
23. Tian Q*, et al.* Mesoporous carbon spheres with programmable interiors as efficient nanoreactors for H_2O_2 electrosynthesis. *Nat. Commun.* **15**, 983 (2024).
24. Zhang X*, et al.* Single zinc atom aggregates: synergetic interaction to boost fast polysulfide conversion in lithium-sulfur batteries. *Adv. Mater.* **35**, 2208470 (2023).
25. Li Z*, et al.* Regulating the N coordination environment of Co single-atom nanozymes for highly efficient oxidase mimics. *Nano Lett.* **23**, 1505-1513 (2023).
26. Ren D*, et al.* Hierarchically porous multimetal-based carbon nanorod hybrid as an efficient oxygen catalyst for rechargeable zinc-air batteries. *Adv. Funct. Mater.* **30**, 1908167 (2020).
27. Yang S*, et al.* Metal single-atom and nanoparticle double-active-site relay catalysts: design, preparation, and application to the oxidation of 5-hydroxymethylfurfural. *ACS Catal.* **12**, 971-981 (2022).
28. Wang Z*, et al.* Understanding the synergistic effects of cobalt single atoms and small nanoparticles: enhancing oxygen reduction reaction catalytic activity and stability for zinc-air batteries. *Adv. Funct. Mater.* **31**, 2104735 (2021).
29. Chen Z*, et al.* Designing a robust palladium catalyst for formic acid dehydrogenation. *ACS Catal.* **13**, 4835-4841 (2023).
30. Liu H*, et al.* Asymmetric coordination of single-atom Co sites achieves efficient dehydrogenation catalysis. *Adv. Funct. Mater.* **32**, 2207408 (2022).
31. Tang C*, et al.* A stable nanocobalt catalyst with highly dispersed CoN_x active sites for the selective dehydrogenation of formic acid. *Angew. Chem. Int. Ed.* **56**, 16616-16620 (2017).
32. Wu N*, et al.* Stabilizing precursor solution and controlling crystallization kinetics simultaneously for high-performance perovskite solar cells. *Adv. Mater.* **35**, 2304809 (2023).

33. Li X*, et al.* Single atom Pd_1/ZIF-8 catalyst via partial ligand exchange. *Nano Res.* **16**, 8003-8011 (2023).

34. Chao S*, et al.* Nitrogen-doped carbon derived from ZIF-8 as a high-performance metal-free catalyst for acetylene hydrochlorination. *Sci. Rep.* **7**, 39789 (2017).

35. Patowary S, Chetry R, Goswami C, Chutia B, Bharali P. Oxygen reduction reaction catalysed by supported nanoparticles: advancements and challenges. *ChemCatChem* **14**, e202101472 (2022).

36. Qiu J*, et al.* Size-controllable synthesis of ZIF-8 and derived nitrogen-rich porous carbon for CO_2 and VOCs adsorption. *ChemistrySelect* **7**, e202203273 (2022).

37. Li J*, et al.* Selective etching of metal-organic frameworks for open porous structures: mass-efficient catalysts with enhanced oxygen reduction reaction for fuel cells. *J. Am. Chem. Soc.* **145**, 27262-27272 (2023).

38. Wang M*, et al.* Interfacial water activation by single-atom Co–N_3 sites coupled with encapsulated Co nanocrystals for accelerating electrocatalytic hydrogen evolution. *ACS Catal.* **12**, 10771-10780 (2022).

39. Han X*, et al.* Hollow mesoporous atomically dispersed metal-nitrogen-carbon catalysts with enhanced diffusion for catalysis involving larger molecules. *Nat. Commun.* **13**, 2900 (2022).

40. Ban J*, et al.* Dual evolution in defect and morphology of single-atom dispersed carbon based oxygen electrocatalyst. *Adv. Funct. Mater.* **31**, 2010472 (2021).

41. Zhang C*, et al.* Enabling logistics automation in nanofactory: cobalt phosphide embedded metal-organic frameworks for efficient electrocatalytic nitrate reduction to ammonia. *Adv. Mater.* **n/a**, 2313844 (2024).

42. Wang Q*, et al.* Evolution of Zn(II) single atom catalyst sites during the pyrolysis-induced transformation of ZIF-8 to N-doped carbons. *Sci. Bull.* **65**, 1743-1751 (2020).

43. He Y*, et al.* Single cobalt sites dispersed in hierarchically porous nanofiber networks for durable and high-power PGM-free cathodes in fuel cells. *Adv. Mater.* **32**, 2003577 (2020).

44. Chang J*, et al.* Interface synergism and engineering of Pd/Co@N-C for direct ethanol fuel cells. *Nat. Commun.* **14**, 1346 (2023).

45. Hu Z Y, Luo L H, Shang C, Liu Z P. Free energy pathway exploration of catalytic formic acid decomposition on Pt-group metals in aqueous surroundings. *ACS Catal.* **14**, 7684-7695 (2024).

46. Zhou C*, et al.* Immobilizing Pd nanoparticles on amine-functionalized yolk-shell mesoporous silica nanospheres for efficient H_2 production from formic acid dehydrogenation. *Appl. Catal. B* **346**, 123750 (2024).

47. Martin C, Quintanilla A, Vega G, Casas JA. Formic acid-to-hydrogen on Pd/AC catalysts: Kinetic study with catalytic deactivation. *Appl. Catal., B*. **317**, 121802 (2022).

48. Lang S, Yu S H, Feng X, Krumov MR, Abruña HD. Understanding the lithium-sulfur battery redox reactions via operando confocal Raman microscopy. *Nat. Commun.* **13**, 4811 (2022).

49. Liu Y*, et al.* Rhodium nanoparticles supported on silanol-rich zeolites beyond the homogeneous Wilkinson's catalyst for hydroformylation of olefins. *Nat. Commun.* **14**, 2531 (2023).

50. Zhang A, Xia J, Yao Q, Lu Z H. Pd-WO_x heterostructures immobilized by MOFs-derived carbon cage for formic acid dehydrogenation. *Appl. Catal. B* **309**, 121278 (2022).

51. Wang J*, et al.* Covalent triazine framework encapsulated ultrafine PdAu alloy nanoclusters as additive-free catalysts for efficient hydrogen production from formic acid. *ACS Catal.* **13**, 5135-5146 (2023).

52. Qin X*, et al.* Mechanistic analysis-guided Pd-based catalysts for efficient hydrogen production from formic acid dehydrogenation. *ACS Catal.* **10**, 3921-3932 (2020).

53. Wang Z*, et al.* Ultrasmall PdAu alloy nanoparticles anchored on amine-functionalized hierarchically porous carbon as additive-free catalysts for highly efficient dehydrogenation of formic acid. *Appl. Catal. B* **291**, 120140 (2021).

54. Bulut A*, et al.* MnO_x-promoted PdAg alloy nanoparticles for the additive-free

dehydrogenation of formic acid at room temperature. *ACS Catal.* **5**, 6099-6110 (2015).

55. Shi Y*, et al.* Solution-phase synthesis of $PdH_{0.706}$ nanocubes with enhanced stability and activity toward formic acid oxidation. *J. Am. Chem. Soc.* **144**, 2556-2568 (2022).

56. Hou T*, et al.* Modulating oxygen coverage of $Ti_3C_2T_x$ MXenes to boost catalytic activity for HCOOH dehydrogenation. *Nat. Commun.* **11**, 4251 (2020).

REVIEWERS' COMMENTS

Reviewer #1 (Remarks to the Author):

After the revision of the review manuscript and suporting information, in where the authors have made a great job directing all the referee`s comments and improving the first draft. This reviewer considers, that the manuscript can be sent for publication in Nature communication.